Todo list

Evaluating Statistical Methods for Nuclear Forensics Analysis

by

Arrielle C. Opotowsky

A preliminary report submitted in partial fulfillment of

the requirements for the degree of

Doctor of Philosophy

(Nuclear Engineering & Engineering Physics)

at the

UNIVERSITY OF WISCONSIN–MADISON

November 2017

Preliminary Examination Committee:

Rebecca M. Willet, Professor, Electrical & Computer Engineering

Charles F. Weber, Distinguished Scientist, Oak Ridge National Laboratory

Jake P. Blanchard, Professor, Nuclear Engineering & Engineering Physics

Douglass L. Henderson, Professor, Nuclear Engineering & Engineering Physics

Paul P.H. Wilson, Professor, Nuclear Engineering & Engineering Physics

For Steve

ACKNOWLEDGMENTS

This proposal would not be possible with the wisdom and patience of my advisor, Paul Wilson. May you never suffer another student like me. I'm also appreciative of the CNERG community for technical and non-technical assistance; may quiche recipes be forever shared during important phone calls. Kelly Burton and Max Lagally have invested **much** effort into my success and convinced me to remain on the graduate school path—more than once. This material is based upon work funded by the National Science Foundation Graduate Fellowship Program, as well as the United States (US) Department of Homeland Security (DHS) under Grant Award Number 2012-DN-130-NF0001.[1]

Mountains of personal support motivated me here and kept me here, which I do not take for granted. Steven "If you're gonna be dumb you gotta be tough" Harrell, my chosen father, pushed me to get all my KSAs via grad school. My GERS friends have motivated me since the beginning, especially José Roberto, Richard, and Chandler. Robin, you have been such a light in my life for over a decade and always remind me why I came back to grad school. And to my friends for 15 years, Denise and April, thanks for keeping in touch despite the gaps. Also, Ruthie, you push me to be fierce, spittin' truths and slaying your way through life. And my family; although enormous, some fought with and for me during grad school. Maurice, thanks for the help when I was struggling. Lou, thanks for being one of my best friends and sources of laugh lines. Liz, make good choices. For tirelessly encouraging my academic and personal pursuits, I'm appreciative of my California family, Mel, Bonnie, Joelle, and Jamie.

Finally, my Madison family has blessed me in countless ways: Shan, Krystal, Ninja, Peter, Drax, Samira, Heather, Burnie, Brarit, Sarah, the late Otto, James, Troy, BLou, Fetal, Corey, Martha, Matt.

[1]The views and conclusions contained in this document are those of the author and should not be interpreted as representing the official policies, either expressed or implied, of the US DHS.

CONTENTS

LIST OF TABLES

LIST OF FIGURES

ABSTRACT

Nuclear forensics is a nuclear security capability that is broadly defined as material attribution in the event of a nuclear incident. Improvement and research is needed for both technical and non-technical components of this process. One such technical area is the provenance of non-detonated special nuclear material (SNM); studied here is spent nuclear fuel (SNF), which is applicable in a scenario involving the unlawful use of commercial byproducts from nuclear power reactors. The experimental process involves measuring known forensics signatures to ascertain the reactor parameters that produced the material. Knowing these assists in locating the source of the material. This work is proposing the use of statistical methods to determine these quantities instead of empirical relationships.

The purpose of this work is to probe to what extent this method is feasible. Thus, three experiments have been designed, using nuclide vectors as observations and simulation inputs as the prediction goals. First, machine learning algorithms will be employed with full-knowledge training data, i.e., nuclide vectors directly from simulations. Second, this workflow will be performed on reduced-knowledge training data, analgous to a detector that can only measure certain radionuclides. Third, these two experiments will then include recycled nuclear fuels to evaluate the methodology when many chemical and elemental signatures are lost in processing. The results will be evaluated using both the prediction accuracy and confidence.

1 INTRODUCTION

The realm of nuclear security involves parallel efforts in nonproliferation (verification of treaty compliance, monitoring for smuggling, proper storage and transportation of nuclear materials), cyber security, minimizing stocks of weaponizable materials, disaster response training, and nuclear forensics. All of these efforts have been continually improving, but there was a gap regarding the ability of the US to coordinate and respond to a nuclear incident, especially with the technical portion of nuclear forensics: characterization and analysis. After all, the first textbook on the topic was published in 2005 [18]. In 2006, the US DHS founded the National Technical Nuclear Forensics Center (NTNFC) within the Domestic Nuclear Detection Office (DNDO). The mission of the NTNFC is to establish a robust nuclear forensics capability to attribute radioactive materials with demonstrable proof.

Multiple fields contribute to a nuclear forensics capability, such as radiochemical separations, material collection techniques, detector technology, material library development, and identifying forensic signatures. These needs vary based on whether the material being collected is post-detonation (e.g., bomb debris) or pre-detonation (e.g., spent nuclear fuel (SNF)). In the pre-detonation realm, this project focuses on statistical methods to to model SNF production history using nondestructive detector measurements.

1.1 Motivation

Nuclear forensics is an important aspect of deterring nuclear terrorism even though it is not, at first glance, obvious preventative nuclear security. The most common defense of the field is that nuclear forensics deters state actors, not terrorist organizations. While it is true that a strong capability encourages governments to be more active in prevention of nuclear terrorism, it can also deter the terrorist organizations as well by increasing their chances of failure. Small destructive successes tend to be more valued than high-risk mass destruction. Nuclear forensics can also assist in cutting off certain suppliers of nuclear materials or technologies (e.g., nuclear specialists that are only involved for financial reasons, access to state suppliers), building a concrete barrier to nuclear terrorism. Therefore, nuclear forensics is considered impede nuclear terrorism in both tangible and abstract ways [16].

Following the prevention value of nuclear forensics, it is important to understand the process of the technical portion of the investigation and how that can be improved. In the event of a nuclear incident, such as the retrieval of stolen SNM or the detonation of a dirty bomb, it is necessary to learn as much as possible about the source of the materials in a timely manner. In the case of non-detonated SNM, knowing the processes that produced it is crucial to determine the chain of custody of the interdicted material. Section 1.1.1 covers the specific needs of the nuclear forensics community for SNF provenance, and Section 1.1.2 discusses how computational approaches

are useful, with a focus on why statistical methods in particular are being pursued.

1.1.1 Needs in Nuclear Forensics

The process of technical nuclear forensics includes the analysis and interpretation of nuclear material to determine its history, whether that be intercepted SNF, uranium ore concentrate (UOC), or the debris from an exploded nuclear device. After the technical portion is complete, intelligence data is used to aid in material attribution; this is the overall goal of nuclear forensics.

After a nuclear incident, the material or debris is sampled and evaluated through many techniques that provide the following information: material structure, chemical and elemental compositions, and radioisotopic compositions and/or ratios. These measurements or ratios comprise the forensic signatures of the sample in question. These signatures can be analyzed with specific domain knowledge; for example, UOC will have trace elements depending on where it was mined from. They can also be analyzed against a materials reference database in the case of SNF.

Measurement needs and techniques vary vastly depending on the material, as does the type of signature. This study focuses on non-detonated materials, specifically, SNF. Tracing the source to an entity or state depends on determining if some intercepted SNF is from an undisclosed reactor or a commercial fuel cycle. This is typically done by obtaining select chemical and

elemental signatures and isotopic ratios, and comparing these measurements to those in an existing forensics database of reference SNF. The signatures for SNF correlate to characteristics that can, in a best case scenario, point to the exact reactor from which the fuel was intercepted. The reactor parameters of interest are the reactor type, fuel type, enrichment at beginning of irradiation, cooling time, and burnup [1, 32, 33].

The current and future work of this study are designed based on two primary needs to bolster the US nuclear forensics capability: post-incident rapid characterization, and forensics database challenges and imperfection.

First, our best measurement techniques cannot be available in an emergency scenario, and fast measurements typically yield inaccurate results. Currently, both radiological measurements and mass spectrometry are used in nuclear forensics exercises. Because these techniques have a multitude of variants within each category, there are differing levels of measurement uncertainties. A lofty goal would be to develop methods that provide instantaneous information, reliable enough to guide an investigation (e.g., within 24 hours). In the case of SNF, it takes weeks in a lab to measure isotopes via advanced (cooled detector) gamma spectroscopy and mass spectrometry equipment. A handheld detector that measures gamma spectra could provide the fast measurements to calculate isotopic ratios for the above-mentioned fuel parameters of interest. However, while this nondestructive analysis is rapid, it is also difficult to evaluate because of the presence of overlapping peaks and the fact that uncertainties differ significantly because

of the detector reponse, environment, storage, electronics, etc. Broadly speaking, there is a time/cost and information tradeoff: gamma spectra give less information at a higher uncertainty than the near-perfect results of the destructive mass spectrometry techniques used for characterization, such as inductively coupled plasma mass spectrometry [11].

Second, forensics databases are imperfect; this is three-fold. Because of the values needed for material provenance, forensics databases are highly multidimensional. Also because of the number of measurement types, the forensics databases have inconsistent uncertainties or missing data entries [12]. Thus, direct comparison between measurement results and a database therefore may not yield accurate parameter predictions. Furthermore, these databases are kept by individual countries, and the reactor operation history information is well-guarded, so it may be difficult to study SNM from a country that has a different fuel cycle. It is proposed that using an machine learning (ML) model with simulated SNF may be able to combat these issues; this is introduced next in Section 1.1.2.

1.1.2 Contribution of Statistical Methods

As previously mentioned, there are two main issues that are being addressed for forensics of SNF: database issues and speed of characterization. Many have begun considering computational techniques developed by nuclear engineers to calculate the parameters relevant to nuclear forensics analysis. One example is the INverse DEPletion THeory (INDEPTH) tool [1, 32, 33].

INDEPTH uses an iterative optimization method involving many forward simulations to obtain reactor parameters of interest given some initial guesses.

Another approach utilizes artificial intelligence (AI) to solve nuclear forensics problems, such as implementing searching algorithms for the database comparison step [5] or ML for determining reactor parameters from SNF characteristics [3, 9, 10, 19, 21, 22, 26, 27]. A variety of statistical and ML tools have been used to characterize SNF by predicting categories (e.g., reactor type, fuel type) as well as predicting values (e.g., burnup, initial enrichment, cooling time). The former uses classification algorithms and the latter uses regression algorithms, many of which can be altered to perform both classification and regression.

Statistical methods have the uniqueness of requiring minimal domain knowledge via ML algorithms that predict the characteristics or values of interest [3, 9, 10, 19, 21, 22, 26, 27]. They first create a black-box statistical model using the entries of measurements in a database. From that, they can predict the reactor parameters of an unknown sample based on that model. Having an ML model based on a large number of simulations may also overcome the challenges of missing data, irregular uncertainty, or lack of information on other fuel cycles. This logic also follows for other computational methods using a large number of simulations. Although they may not involve a resuable model, they also could overcome missing data, irregular uncertainties, or ignorance of different or non-commercial fuel cycles. Also, it is generally known that statistical methods will be able

to either use or reduce the dimensions in the forensics databases, which is another useful characteristic.

1.2 Methodology

As previously mentioned, the typical workflow of the technical portion of a forensics investigation is to analyze measurements of an unknown material. The measurements are compared to databases filled with previously measured standard materials with known reactor parameters, and/or the reactor parameters are calculated from empirical relationships. As this work focuses on SNF, these measurements are elemental, chemical, and radiological in nature. Because creating databases from real measurements to represent SNF from reactor technologies from around the world is not within the scope of this project, the database in this study will be created from high-fidelity simulations via the Standardized Computer Analyses for Licensing Evaluation (SCALE) [23] system using Oak Ridge Isotope GENeration (ORIGEN) [25].

To understand how a physics-free model can predict nuclear reactor parameters, Figure 1.1 introduces the INDEPTH and statistical methodologies, both of which use simulated SNF. While not all steps are required to be equivalent, the only difference here is the method one chooses to obtain reactor parameters. Both workflows address speed of characterization, as it is intended to have gamma spectra as the inputs. Because INDEPTH

is better studied and validated than statistical methods [1, 32, 33], this work focuses on a statistical approach but with the intention to compare methodologies. Both workflows also address many of the database issues, described above. The statistical methodology is described below.

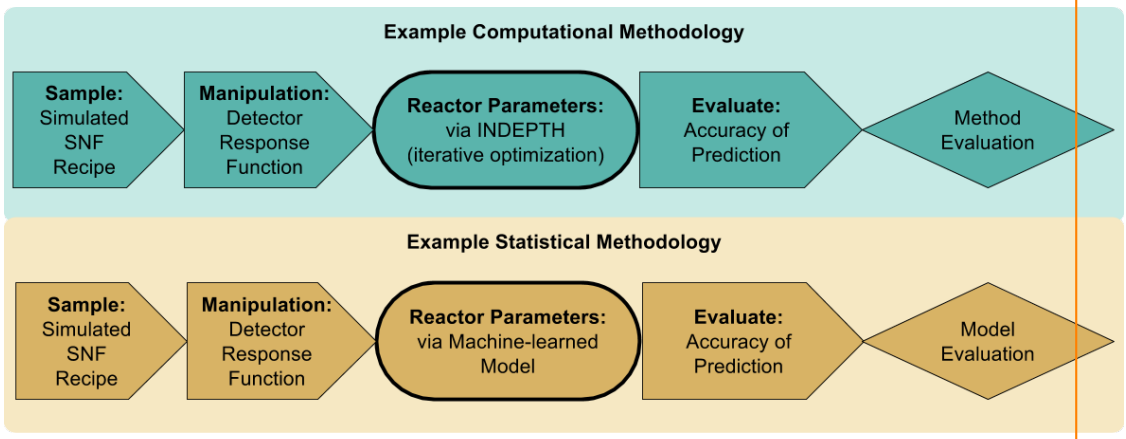

Figure 1.1: Computational Forensics Research Workflows

could simplify this figure a lot

In the simulation and statistical learning paradigm, we need to determine how much information to what quality is needed to train an ML model; the model must give appropriate predictions of reactor parameters given a set of measurements from a *test* sample.

The next step is to choose an algorithm that performs statistical learning. Statistical learners have varied strengths and weaknesses based on what is being predicted and how they implement optimization. Chosen for this study are simple regression algorithms for burnup prediction: nearest neighbor and ridge regression. For comparison, support vector regression (SVR) is

used because it is known to handle highly dimensional data sets well. These algorithms are introduced in Section 2.2.1.

After the training is complete, the results of each models' predictions must be evaluated according to ML best practices. The machine-learned model predicts the parameters of a previously unseen test set. The difference between the model predictions and the actual simulated parameters is known as the testing error. The testing error with respect to various specifications such as the training set size, number of features, or algorithm parameters provides insight into the model performance. These results are broadly known as diagnostic plots and show if the predictions are due to good performance or bad fitting.

After the models are evaluated, it will be important to compare them both against each other and against other computational forensics methods. Thus, a Bayesian approach from the field of inverse problem theory will be used to give the probability distribution of the predictions so that the statistically generated predictions can be evaluated directly against other solutions, such as the optimization-based method, INDEPTH.

Next, information reduction (within the training and testing data sets) must be used to investigate the extension of this workflow to the real world. The primary example here is the reduction of information quality via gamma ray detectors. If an algorithm could overcome the limitations of gamma detection and still provide useful results, this would warrant further studies and perhaps be field-applicable.

Thus, ultimately, the goal is to answer the question *How does the ability to determine forensic-relevant spent nuclear fuel attributes using machine learning techniques degrade as less information is available?*.

1.3 Goals

The main purpose of this work is to evaluate the utility of statistical methods as an approach to determine nuclear forensics-relevant quantities as less information is available. ML algorithms are used to train models to provide these values (e.g., reactor type, time since irradiation, burnup) from the available information. The training data is simulated using ORIGEN, which provides an array of nuclide concentrations as the features (X) and the parameters of interest (y) are provided from the simulation inputs. Information reduction is carried out using computationally generated gamma spectra; the radionuclide concentrations from the simulations can be converted into gamma energies, which then undergo a detector response calculation to represent real as-measured gamma spectra as closely as possible. ML best practices are used to evaluate the performance of the chosen algorithms, and inverse problem theory is used to provide an interval of confidence in the model predictions.

The necessary background is covered in Chapter 2. First, an introduction to the broader field of nuclear forensics is in Section 2.1 to place this work in the context of the technical mission areas. After that, a short discussion of

the field of ML, the algorithms used, and validation methods are in Section 2.2. Section 2.3 includes information about the software used to generate the training data and perform the predictions. Lastly, a review of statistical methods being used in studies of forensics analysis is covered next in Section 2.4.

After the existing work is discussed, the methodology and a demonstration of the experimental components is introduced next in Chapter 3. This will cover the simulated training data in Section 3.1, the the details for training models in Section 3.2, and the process of model evaluation in Section 3.3.

Finally, Chapter 4 summarizes the official thesis research proposal. After the preparatory tasks are covered in Section 4.1, there are three experiments outlined in Sections 4.2, 4.3, and 4.4. Qualitiative hypotheses as well as alternative directions for risk mitgation are discussed throughout these sections. A detailed explanation of the method comparison step is covered next in Section 4.5. Lastly, a projected timeline for the completion of this project is in Section 4.6.

2 BACKGROUND AND LITERATURE REVIEW

This chapter provides background and a literature review of the necessary components for this project. Section 2.1 outlines the broader field of technical nuclear forensics, with a focus on the area that motivates this project. Section 2.2 introduces the field of machine learning for an uninitiated audience, covers the relevant algorithms, and presents the methods field practitioners use for validation. Next, Section 2.3 covers the computational methods used to generate the training data for the ML input. Finally, the marriage of Sections 2.1, 2.2, and 2.3, is presented in Section 2.4, which is a review of previous work applying statistical methods to the nuclear forensics analysis of pre-detonated nuclear materials.

2.1 Nuclear Forensics

Nuclear forensics comprises a large part of an investigation into a nuclear incident, such as interdicted nuclear material or the detonation of a weapon containing radioactive components. The forensics portion of the investigation encompasses both the analysis of nuclear material and/or related paraphrenalia as well as the interpretation of these results to establish nuclear material provenance. The former has many technical aspects, relying on a range of nuclear science and chemistry. The latter involves intelligence and political considerations of the material analyses for attribution. This review

will only consider the technical portion of the nuclear forensics workflow.

First discussed are the types of forensic investigations in Section 2.1.1, followed by an introduction to inverse problem theory in Section 2.1.2 as a way to evaluate the results of forensic methods.

2.1.1 Types of Nuclear Forensics Investigations

The technical programs researching improvements to the US's nuclear forensics capabilities are split between the type of material being investigated. The analysis of irradiated debris from a weapon has different collection and measurement requirements than a mass of SNM. This separates the field into post-detonation and pre-detonation nuclear forensics. While both are discussed below in Sections 2.1.1.1 and 2.1.1.2, respectively, there is more focus on pre-detonation topics since this work is based on SNF.

2.1.1.1 Post-Detonation

Post-detonation nuclear forensics requires a diverse set of measurements to obtain the following information: identification of nuclear material, reconstruction of the weapon device design, and reactor parameters for nuclear material provenance. This could apply to an improvised nuclear device or a nuclear bomb. In conjunction with the measurements and characterization are a large array of logistical concerns, including recovery efforts, personnel safety, and material collection cataloging and transportation.

In the case of a full explosion using fissile material, the collection of materials and debris occurs as quickly as possible. It can be in the crater created by the explosion, further away from the center in the fallout, and in the atmosphere above or downwind from the detonation. These are collected by finding glass-like material near the epicenter, debris swipes in the fallout region, and advanced particle collection in the atmosphere via an airplane, respectively. While the epicenter cannot be reached for some time, the debris and atmosphere measurements of radioactive material can provide the yield of the weapon and whether it was made using uranium or plutonium. This along with other physical and chemical measurement allow device reconstuction to begin. Attribution begins to narrow to specific countries or organizations based on this information. [16]

The research needs for post-detonation focus on material collection and analysis as well as nuclear device modeling for rescontruction purposes. Ideally, most material sample collection would be done using automatic instrumentation. Additionally, bolstering the existing device modeling code for reverse engineering is needed. And, as with pre-detonation, a database of standard materials must be both strengthened and centralized. [16]

2.1.1.2 Pre-Detonation

Pre-detonation nuclear forensics investigations occur for every scenario in which non-detonated nuclear material has been found or intercepted. Although this could be an intact bomb, it is more likely that SNM intended

for a weapon would be the target of an investigation. Thus, the range of intact materials for measurement could be as small as a plutonium sample or as large as a shipment of UOC. The goal is to determine the provenance of the SNM, which in the case of SNF is generally done by reconstructing the irradiation process that created the material.

For SNF, where the material was obtained is the first step of the investigation. This would be gleaned from the reactor parameters and storage history (e.g., reactor type, cooling time, burnup), which requires first measuring and calculating certain values: isotopic ratios, concentration of chemical compounds, or existence of trace elements. Both radiological methods (e.g., gamma spectroscopy) and ionization methods (e.g., mass spectrometry) measure these quantities.

Although this is less of a humanitarian emergency than a post-detonation investigation, it is still important to have rapid characterization capabilities via on-site non-destructive analyses. As previously discussed in Section 1.1, however, the faster measurements result in poor measurement quality. Also, there is a need for research to combat the database issues, as an insufficient forensics database can reduce the accuracy and/or certainty of a reconstructed set of reactor parameters. Another area of research is deeper study of known forensics signatures or discovering new signatures with modeling, simulation, or statistical methods.

The top panel in Figure 2.1 shows an example technical nuclear forensics workflow as it could occur in the real world for a pre-detonation scenario.

After a sample is obtained, characterization begins. Next, the results of these techniques are then compared against existing standard materials databases to obtain the desired reactor parameters. These steps would be performed iteratively in a real investigation, first using non-destructive measurements, and then destructive measurements. The following steps in Figure 2.1 are seeking out reactor history information, if available, and reporting all results to the investigators.

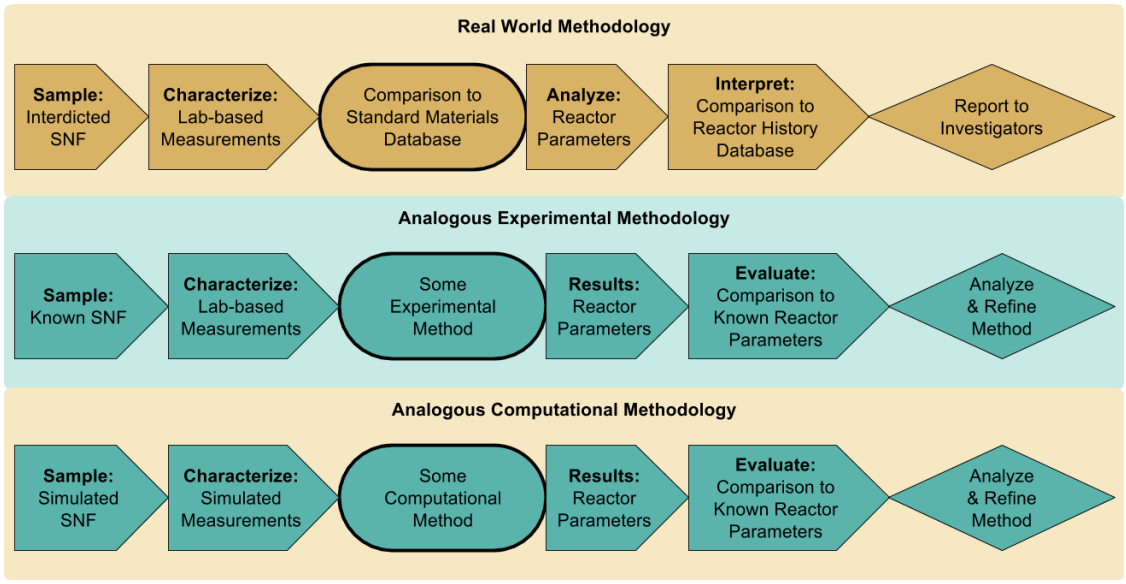

Figure 2.1: Example Forensics Workflows in Real-World Scenario

The middle and bottom panels in Figure 2.1 are analagous physical and computational experimental workflows, respectively. Both panels would have validated measurements of SNF; the middle panel shows this being done in the laboratory and the bottom panel shows that these are values from

a simulation. For studying alternative measurement techniques or a slight difference in the overall approach, a researcher would iterate through multiple studies using known materials to probe sensitivities or other weaknesses in the procedure.

2.1.2 Nuclear Forensics as an Inverse Problem

Nuclear forensics is a traditional inverse problem, which has been well documented mathematically and applied to a range of scientific disciplines. Understanding inverse problem theory can help systematically define the limitations of certain solution methods. This section provides an introduction to the topic as well as its application to nuclear forensics.

As outlined in a textbook on the formal approach to inverse problem theory [30], the study of a typical physical system encompasses three areas:

1. *Model parameterization*
2. *Forward problem:* predict measurement values given model parameters
3. *Inverse problem:* predict model parameters given measurement values

First, this shows that it is important to consider the parameters that comprise a model; this is denoted as the *model space*. This is not every measurable quantity; domain knowledge is necessary to determine the model space. In the nuclear forensics context for SNF, this would consist of, e.g., the cooling time because the SNF decays and material measurements are different depending on when the measurement is taken.

Second, understanding the physical system also requires an understanding of the forward problem. Predicting how a certain set of values of model parameters will affect the resulting measurements is a problem with a unique solution. The breadth of these end measurements provides the *data space*, which are all the conceivable results of a given forward problem. So for SNF this would be, perhaps, the range of isotopic ratios typical of a commercial reactor.

Lastly, the inverse problem is predicting the model parameters given a solution. It is statistical in nature; there is a probability that the measured isotopes are caused by some value of a model parameter. Thus, the problem is *ill-posed* because a prediction is not guaranteed to be unique.

Further, including measurement uncertainties broadens the linear model to probability densities of the parameters. The opposite is also true in the forward case: including parameter uncertainties broadens the forward problem results to probability densities of the potential measurement values. [30]

In this way, we can define some probability that an answer is correct, given a set of measurements and their uncertainties, the calculated model parameters, the spread of the data space, and the spread of the model space. Inverse problem theory connects these values to the general form of Bayes' theorem, which is commonly expressed as follows:

$$P(A|B) = \frac{P(B|A)P(A)}{P(B)} \tag{2.1}$$

Here, A and B are events, $P(A)$ and $P(B)$ are the probabilities that events A and B will occur, representing the model and data spaces, respectively. $P(A)$ is known as the likelihood and $P(B)$ is known as the marginal likelihood. The marginal likelihood is a concept of the data space capturing all the possible measurement values. It is ignored here because as a homogenous probability, it is only useful for determining absolute probabilities and this will only be applied in a relative context. $P(B|A)$ is the prior probability that event B will occur given a known result for A, which are the measurements given the model parameters (i.e. the forward problem). $P(A|B)$ is the posterior probability that event A will occur given a known result for B, which are the predicted model parameters given the measurements (i.e., the inverse problem) [29, 30]. A discussion of how these values are obtained takes place in Section 2.2.3.3.

Given the above, it is more intuitive to consider the conceptual version of Bayes' theorem in Equation 2.2.

$$Posterior = \frac{Likelihood * Prior}{Marginal\ Likelihood} \tag{2.2}$$

This framework is helpful for an experiment that intends to compare different methods for calculating the posterior probability of a system given some measurements [31]. In the nuclear forensics context of pre-detonated materials, this would be a a set of probabilities for different parameters of interest, e.g., reactor type, burnup, cooling time, and enrichment of some

interdicted SNF.

2.2 Machine Learning

Machine learning (ML) is a sub-field of AI within the broad category of computer science. The goal of AI is to create computer systems that respond to their environment according to some set of criteria or goal [13]. For example, self-driving vehicles have computers on board that learn to avoid curbs and humans. While its use has been increasing in the commercial sector, there is also much anecdotal evidence to support the existence of a rapid increase of AI use in academic research across many disciplines beyond robotics. AI systems have been used in detection (e.g., fraud or spam), medical diagnostics, user analysis (e.g., Netflix ratings), and a host of scientific disciplines that have increasing amounts of multivariate data.

ML research focuses on the underlying algorithms using mathematical optimization, methods for pattern recognition, and computational statistics. Much of the recent advances to the field of AI have occured in the statistical realm, which forgoes domain knowledge in favor of large data sets. In this work, there is no distinction made between the terminology of machine learning and statistics. Additionally, this study is not concerned with computational time, but rather the ability to correctly predict values and categories relevant to the nuclear forensics mission. This restricts the relevancy of the algorithms to the underlying theory and its impact on the

resulting model's accuracy.

ML algorithms can be separated into two main categories: unsupervised and supervised learning. The former groups or interprets a set of input data, predicting patterns or structures. The latter includes both the input and output data, enabling the ML model to predict future outputs. Broadly speaking, the unsupervised learning algorithms are designed for clustering data sets or dimensionality reduction (i.e., determining some subset or linear combination of features most relevant to the input data) of data sets. Supervised learning algorithms predict both discrete and continuous values via classification and regression, respectively. Some algorithms can perform both classification and regression, and neural networks can even be modified to perform either supervised or unsupervised learning.[6]

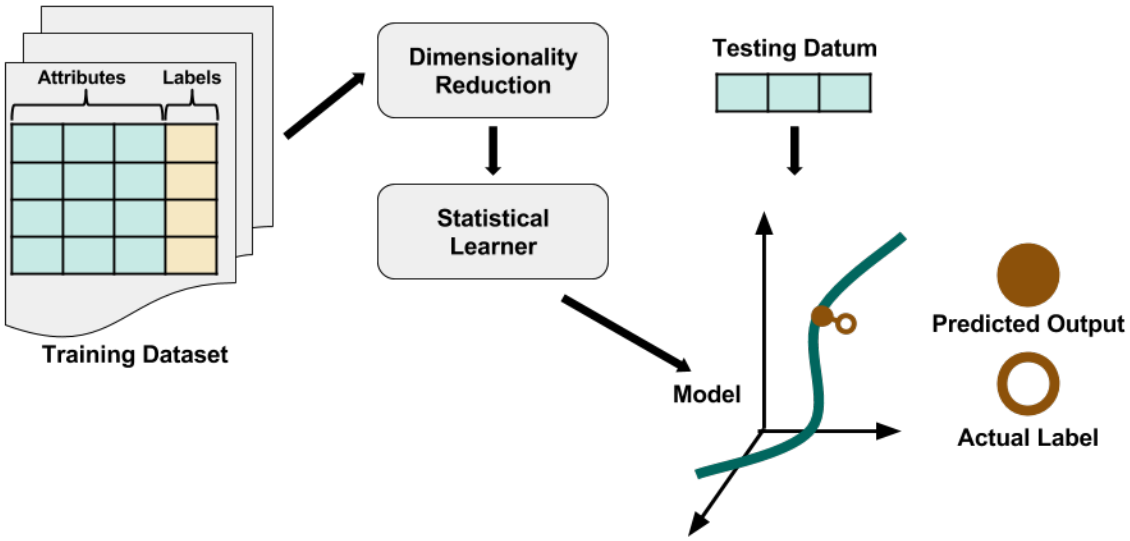

Figure 2.2: Schematic of Regression with Machine Learning

As shown in Figure 2.2, a typical (supervised) machine learning workflow begins with a training data set, which has a number of *instances*, or rows of *observations*. Each instance has some *attributes*, also referred to as *features*. It also has a *label*, which can be a categorical label or discrete/continuous values.

The training data are then inserted into a statistical learner; this calculates some objective, minimizes or maximizes that objective, and provides some model. This model can be evaluated using a testing set that has the same set of features and labels (but different instances). The comparison of what the model predicts and the actual label gives the *generalization error*. Depending on the performance and application, the model may need improvement from more training and/or some changes in the algorithm parameters. Once the model is performing well enough and validated, it is finalized; then a user can provide a single instance and a value can be predicted from that.

This study performs regression tasks using supervised learning algorithms. Differences among the structure underlying mathematics of the algorithms impact the ML models. Therefore, the algorithms used in this study will be discussed in Section 2.2.1. Next, model selection and assessment is covered in Section 2.2.2. Evaluating and optimizing algorithm performance is discussed in Section 2.2.3, as well as robustly comparing different algorithms for validation.

2.2.1 Algorithms for Statistical Learning

For relevant nuclear forensics predictions, both classification and regression algorithms must be used. For example, one may want to predict the reactor type label given some measurement-based features of SNF of an unknown source. This would require a classification algorithm. Or perhaps the input fuel composition is relevant to an investigation on weapons intent, so a regression algorithm would be used to train a model based on some different set of measured features. Since this work trains models to predict burnup of SNF, the algorithms are presented in a regression context.

2.2.1.1 Linear Models

One of the simplest and most utilized methods of prediction is a linear model from a least-squares fit. Thus, it is the most natural place to begin a demonstration of ML algorithms. Since linear models must have all linearly related parameters, there are many restrictions regarding the shape of the model. However, this makes the resulting models stable to peturbations. [13]

An example of a linear model is in Equation 2.3. The vector of input features of size p, $\boldsymbol{X}$, provides a model, $F(\boldsymbol{X})$ by determining the unknown coefficients, or weights, β_j's. A loss function can be calculated by the difference in the model-predicted value and $\boldsymbol{Y}$, the vector of actual labels. The algorithm calculates β_j by minimizing the value of this loss function over all the training data. This is usually the least squares error from minimizing

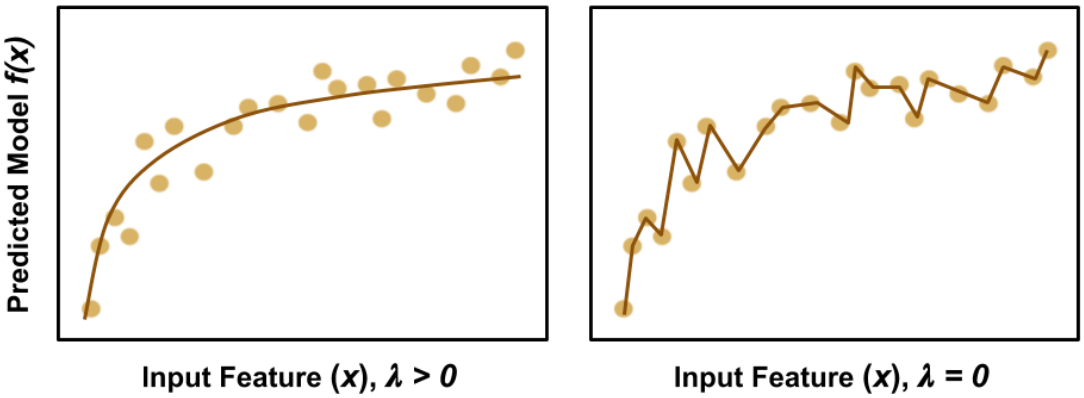

Figure 2.3: Effect of Regularization on Prediction

the sum of squared errors, $\sum_{i=1}^{n}(y_i - f(x_i))^2$. But it could instead be the least absolute deviations from minimizing the sum of absolute error differences, $\sum_{i=1}^{n}|y_i - f(x_i)|$. These are referred to as the L_2 and L_1 norms, respectively.

$$F(\boldsymbol{X}) = \beta_0 + \sum_{j=1}^{p} x_j \beta_j \tag{2.3}$$

The form of linear regression used here is called ridge regression. This algorithm performs optimization using the L_2 norm, and also uses the form of the L_2 norm for *regularization*. Regularization, sometimes called *shrinkage*, is a term introduced into the ML model to prevent overfitting; it is used in many ML algorithms. For ridge regression, shrinkage further reduces the weights, β_j, on the input features, x_j. The shrinkage term also includes a complexity parameter, λ, which governs the strength to which regularization is performed [6]. Thus, the linear model given from ridge regression is updated to Equation 2.4. Figure 2.3 is a visualization of how

applying regularization smooths out a model.

$$F(\boldsymbol{X}) = \beta_0 + \sum_{j=1}^{p} x_j \beta_j + \lambda \sum_{j=1}^{p} \beta_j^2 \tag{2.4}$$

2.2.1.2 Nearest Neighbor Methods

Nearest neighbor regression is a unique algorithm in that it is instance-based; it does not actually generalize, but tracks the observations in the training set. The main metric for this algorithm is distance (or dissimilarity) between the test sample and the closest training sample(s) in the vicinity. During prediction, the algorithm will calculate a value based on the instance that is closest to the current test sample. Thus, there is not any learning, but instead a direct comparison between an unknown sample and the space that the training set populates. The predictions from nearest neighbors can be quite accurate, but are highly unstable to peturbations [6].

An extension of nearest neighbor is k-nearest neighbor regression. The closest k neighbors are averaged for an estimate of the unknown sample, as shown in Equation 2.5. Figure 2.4 provides a pictoral explanation of how this is done for a prediction of a single feature. For k-neighbors, this algorithm predicts a value, Y, from the input features, $\boldsymbol{X}$, in the neighborhood, $N_k(\boldsymbol{X})$ [6].

$$Y(\boldsymbol{X}) = \frac{1}{k} \sum_{x_i \in N_k(\boldsymbol{X})} y_i \tag{2.5}$$

There are two tuneable parameters in this algorithm: the distance metric and the value of k. The population of the neighborhood, k, affects the

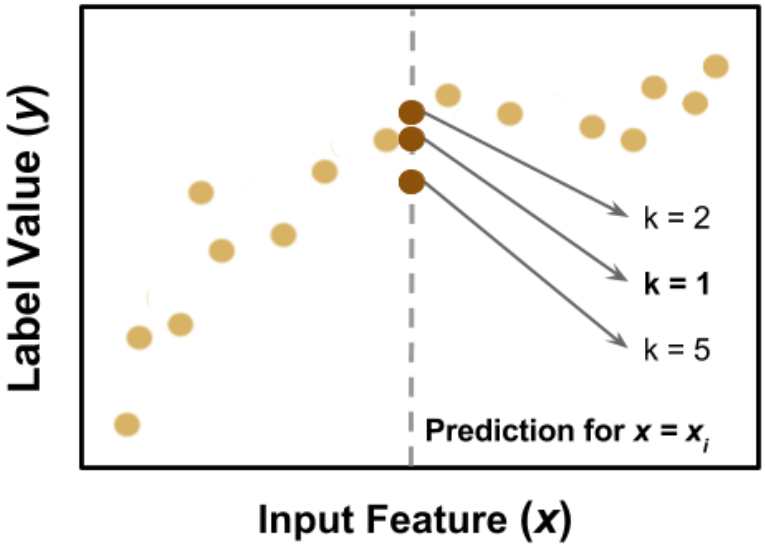

Figure 2.4: Schematic of k-Nearest Neighbors Regression

number of points being averaged together for a prediction. The metrics for distance differ, but in this study, the Euclidian distance was used. In this initial work, $k = 1$ is used. This can perform very well, but can also easily overfit the data and thus not generalize well.

2.2.1.3 Support Vector Machines

Support vector regression (SVR) is an extension of the popular classification algorithm, support vector machine (SVM). This algorithm was chosen because of its ability to handle highly dimensional data well, which in this study is a maximum of approximately 300 features.

As seen in Figure 2.5[1], the support vector machine (SVM) algorithm

[1]This schematic is based on the tutorial on SVMs by Dr. Saed Sayad at http://www.saedsayad.com/support_vector_machine.htm

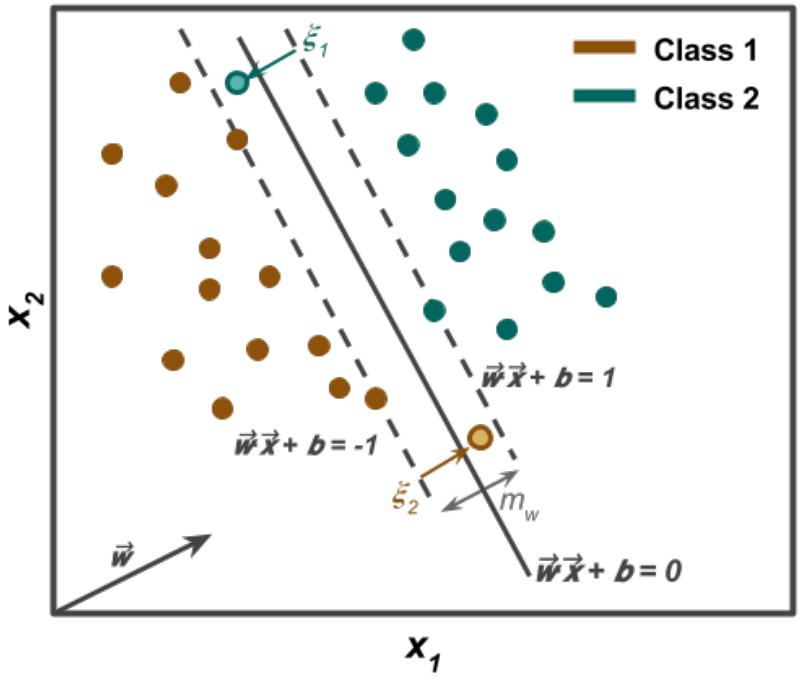

Figure 2.5: Schematic of SVM Classification

separates two classes by determining an optimal hyperplane between them. The algorithm evaluates the quality of the line that separates the two classes by maximizing the margin width, $m_w = \frac{2}{\|w\|}$. The hyperplane is defined in Equation 2.6, where $\boldsymbol{w}$ is the vector that is normal to the hyperplane.

$$\boldsymbol{w} \cdot \boldsymbol{x} + b = 0 \tag{2.6}$$

Figure 2.5 also shows a case of soft margins. Some problems are not linearly separable, and thus a penalty term, ξ_i, is introduced to allow for some misclassifications. The algorithm then simultaneously minimizes the misclassifications while maximizing the margin. The objective function of

the algorithm shows this as well (using quadratic programming) in Equation 2.7. Here, C is responsible for the margin width/misclassification tradeoff, and the penalty term is included in the constraint. [6, 24]

$$\begin{aligned} min\ & \frac{1}{2}\|w\|^2 + C\sum_i \xi_i \\ subject\ to:\ & y_i(wx_i + b) > 1 - \xi_i \end{aligned} \tag{2.7}$$

Figure 2.6[2] demonstrates how SVM can be altered slightly from classification to nonlinear regression with support vector regression (SVR). SVR has a similar objective function but instead *minimizes* the margin, as shown in Figure 2.6a. While the objective function is the same as in Equation 2.7, the constraint is now set to the opposite inequality sign, shown in Equation 2.8

$$\begin{aligned} min\ & \frac{1}{2}\|w\|^2 + C\sum_i \xi_i \\ subject\ to:\ & |y_i - (wx_i + b)| \leq \varepsilon + \xi_i \end{aligned} \tag{2.8}$$

Further, this can be extended to nonlinear analysis via what is called the *kernel trick*. A nonlinear kernel function maps the data into higher order feature space. The algorithm can then find a linear separation in this space, as shown in Figure 2.6b.

Chosen for its flexibility, the kernel in this study is the Gaussian radial basis function, shown in Equation 2.9. This has two tuneable parameters, γ and C. The γ controls the width of influence of individual training instances,

[2]These schematics are based on a tutorial on SVR by Dr. Saed Sayad at http://www.saedsayad.com/support_vector_machine_reg.htm

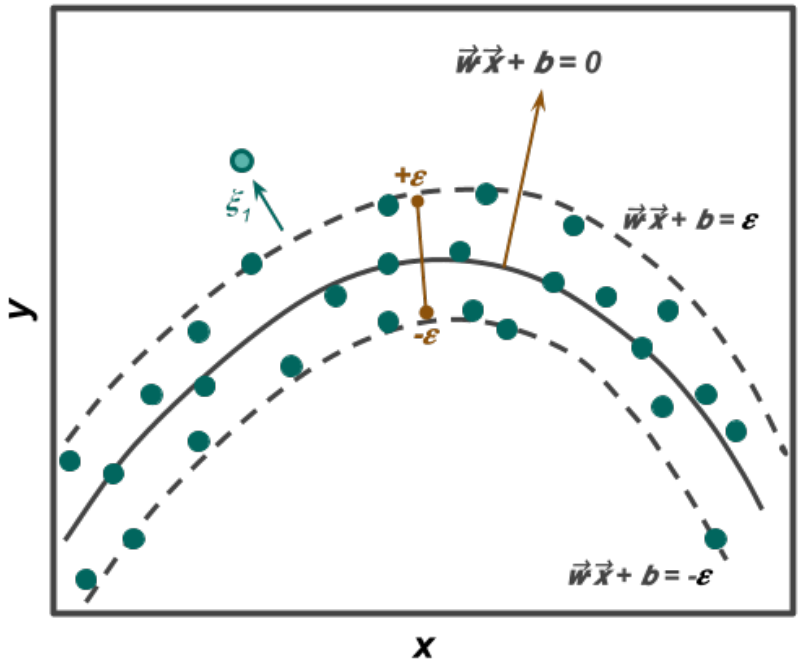

(a) Demonstration of regression with SVR

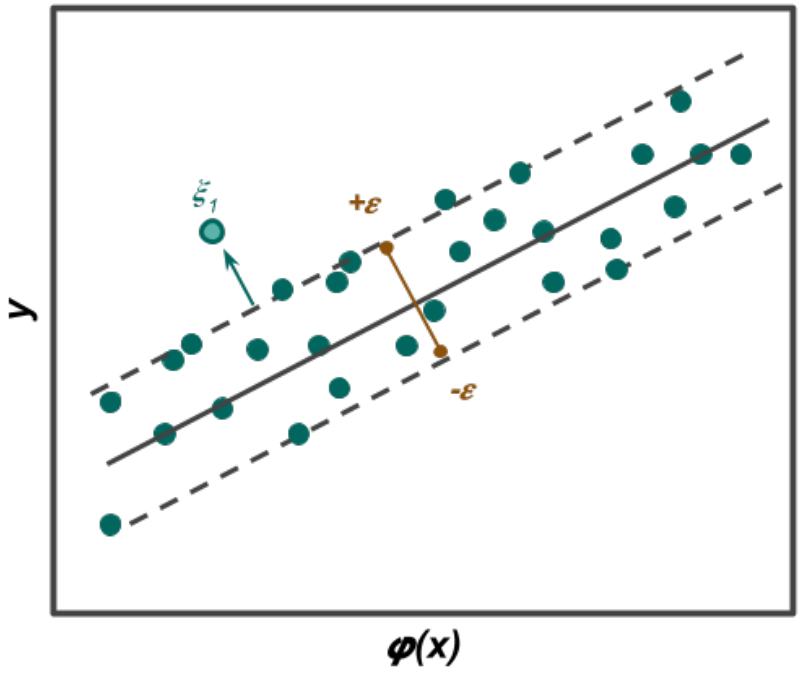

(b) The kernel trick with SVR

Figure 2.6: Illustrations of SVR and Nonlinear Analysis

which strongly affects the fitting of the model. Low values correspond to underfitting because the instances have too large of a radius (low influence) and high values correspond to overfitting because the instances have a small radius (high influence).

$$\begin{aligned} min\ & \frac{1}{2}\|w\|^2 + C\sum_i \xi_i \\ subject\ to:\ & |y_i - (w\phi(x_i) + b)| \leq \varepsilon + \xi_i \\ where: & \ w = \sum_i \alpha_i y_i \phi(x_i) \\ and: & \ K(x_i, x_j) = \phi(x_i)\phi(x_j) = e^{\gamma\|x_i - x_j\|^2} \end{aligned} \tag{2.9}$$

The C parameter also affects the fitting of the model by allowing more or less support vectors, corresponding to more or less misclassification, respectively. A lower C smooths the surface of the model by allowing more misclassifications, whereas a higher C classifies more training examples by allowing fewer misclassifications. Thus, too low or too high of a C can cause under- or overfitting, respectively.

Since there is a tradeoff of fitting strength provided by two parameters, it is common to run the algorithm on a logarithmic grid from 10^{-3} to 10^3 for each parameter. If plotted on a heatmap of accuracies given γ and C, there will be a diagonal of ideal combinations that emerges. The element with the lowest value of each parameter is usually chosen.

2.2.1.4 Dimensionality Reduction Techniques

In addition to utilizing various algorithm parameters for regularization as discussed above, dimensionality reduction can improve generalizability by removing the noise of features that do not affect the regression task. This can be thought of in the following way: shrinkage techniques reduce the weights of noisy features, whereas dimensionality reduction removes them completely [6]. Although one could use domain knowledge to manually reduce the number of features in a data set (e.g., only including certain nuclide subsets such as actinides), statistical feature reduction may also prove helpful in this work. The mathematical treatment of the methods described below are in Ref. [6].

Principal Components Analysis

Principal components analysis (PCA) is considered the most common dimensionality reduction technique. The PCA algorithm learns a linear transformation of a data set $\boldsymbol{X}$ with which to construct a transformation matrix according to a user-chosen number of variables, i.e., components. This matrix is part of the singular value decomposition of the data matrix $\boldsymbol{X}$. The decomposition step is what provides the principal components, which are the result of maximizing the variance in the original data while minimizing the squared reconstruction error between the original data and the transformed data. The mathematical assumptions are that the variables

are all Gaussian and uncorrelated.

Because the principal components are obtained purely statistically with no model assumptions, they are usually uninterpretable. However, they can still provide clues with which to obtain new information. In the case of this work, this could provide insight into new forensics signatures.

Factor Analysis

Factor analysis is similar to PCA in that it also calculates linear combinations of the data set features using the above-mentioned decomposition and the mathematical assumptions are the same. It is different in that the decomposition is rearranged so that it represents *latent variables* including random error disturbances rather than principal components. Latent variables are constructed by maximizing the correlation/shared variance among the variables rather than the total variance. However, different optimizations can be chosen so that the solutions are parameter-dependent.

Furthermore, the initial model assumptions, while enabling interpretable results, also increase the dependence of the solutions on the algorithm inputs. If PCA does not perform well with the type of training data in this work, it is possible that factor analysis will, since there are many nuclides in the training data set that are in a decay chain together.

Independent Components Analysis

Independent components analysis (ICA) has characteristics of both factor analysis and PCA, but with the goal of finding independent measurements from multiple 'sources'. It uses the same form of decomposition as factor analysis but without the inclusion of random error. The mathematical assumptions are a bit different: the variables are statistically independent and non-Gaussian. This allows the algorithm to minimize higher-order statistics of the data set (PCA and factor analysis only minimize the first two orders).

Since the independent components are useful in signal processing of multiple signals, this technique could prove useful for reprocessed nuclear materials where multiple source streams converge.

2.2.2 Model Selection and Assessment

After a model is trained, the first step is model selection and assessment. Selection is estimating model performance among a set of ML models using a single validation set. After one model is chosen, assessment takes place by determining the prediction capability on new data via a previously unseen testing set. Both selection and assessment can be done in a single step using k-fold cross-validation, which is described below.

2.2.2.1 Sources of Error

In statistical learning, there are two sources of error that need to be simultaneously minimized: bias and variance. Bias is caused by simplifications in

the model, so the error is caused by missed relationships in the data; high bias is an indication of an underfit model. Variance is caused by including random noise in the model, so the error is caused by oversensitivity to that noise; high variance is an indication of an overfit model.

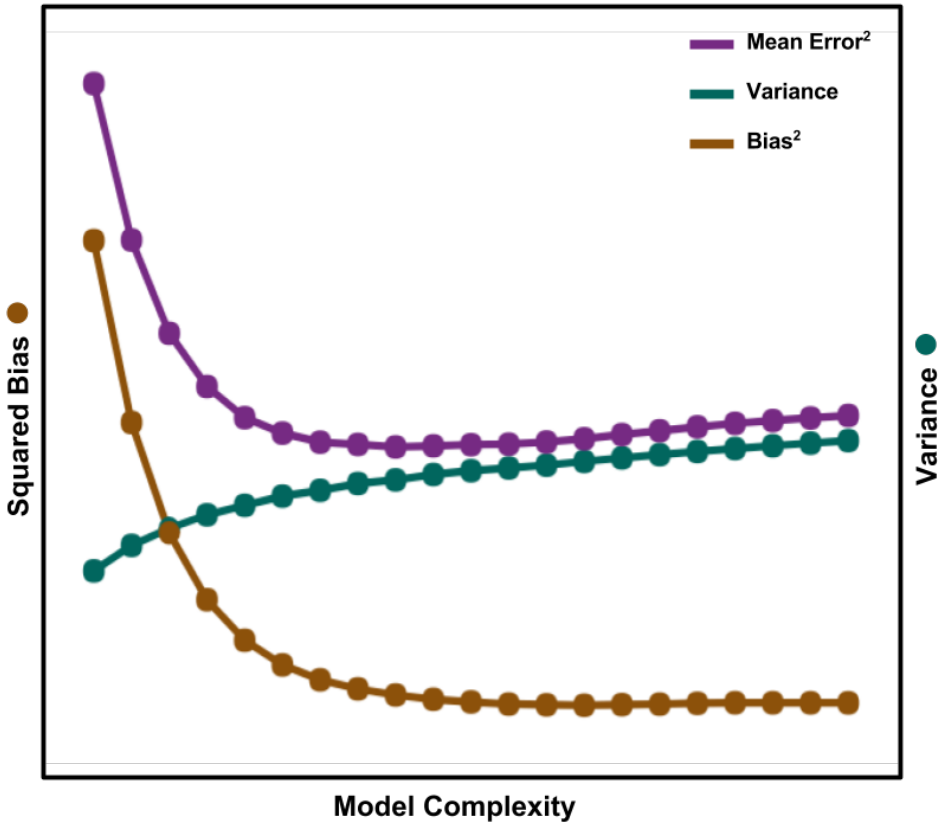

Figure 2.7: Bias and Variance Comprising Prediction Eror

Figure 2.7 shows the tradeoff between the bias and variance. The shape of the total error curve has a minimum that we seek to achieve with our model. Some bias is desired in order to generalize to future unknown data. But some variance is also positive for the model because it captures the

relationships in the data that the bias counteracts.

2.2.2.2 Types of Error

While the sources of the model prediction error are well known, the creation of an ML model is a hidden process. Although the model emerges from a black box, there are ways to evaluate the generalization (i.e., prediction) capability of it. This is done by removing a small portion of the data for use as a testing set. The rest of the data set is known as the training set and is used to train a model. After training, the test set is used to calculate the model's generalization error.

Thus, the generalization error is typically referred to as the *testing error*, as it is measuring the ability of the model to predict future cases that were not introduced in the training phase. Next, the *training error* is provided by comparing the model predictions to the training set, as the model would likely be smoother than the potential noise the training set would include. This is useful to determine the fitness of the model, the application of which is discussed below in Section 2.2.3.

Although one could just train and test their model, there is a way to check the model while still in the training phase. A testing set that would be used during training to give feedback, a *cross-validation* set, can provide a faster convergence to a satisfactory model. As shown in Figure 2.8, this can be done by splitting the data set into three groups: a large training set, a small cross-validation set, and a small testing set. However, in practice, multiple

rounds of cross-validation steps are used provide the fastest convergence. This is referred to as *k-fold cross-validation* and allows a user to have all training data entries be a testing entry once, bettering model evaluation.

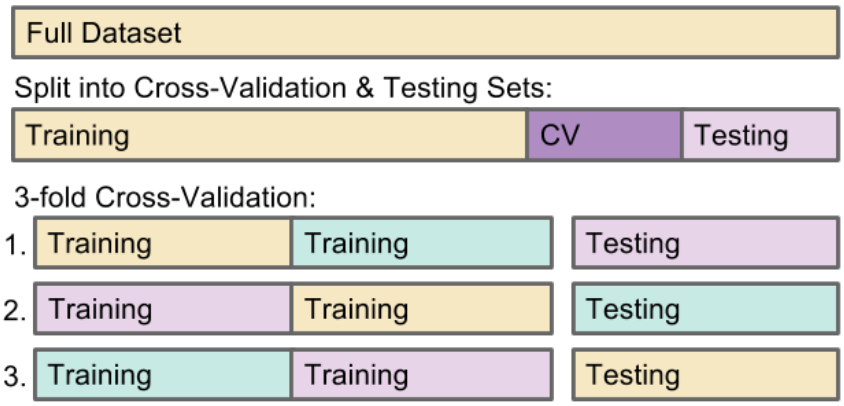

Figure 2.8: Illustration of Cross-Validation

Using cross-validation provides a *cross-validation* error that replaces the testing error during analysis. As illustrated in Figure 2.8, this splits the dataset into $k = 3$ subsets. One set is designated as the testing set, and a model is trained with the rest. Following the first training phase, another begins, this time with a different subset as the testing set. In total, this process in Figure 2.8 is performed 3 times, giving 3 models. The metrics of model performance are averaged by taking the mean of the accuracy/error of predictions. This provides an additional level of model validation than can be achieved with a single testing set. This mean is reported as the cross-validation error. If the cross-validation error is acceptable, then training is performed on the entire training data set and can be tested on new

observations.

2.2.3 Model Optimization and Validation

It is unlikely to have a model perform as one expects the first time. There are therefore a few techniques for optimizing the performance. It should be noted that much of the discussion here and in Section 3.3 focuses on the diagnostics aspect rather than the validation aspect of these techniques. In practice, these are used for both purposes: diagnosing fitness problems and proving good fitness. But in this work the formal comparison of model performance will be used, introduced and detailed in Sections 2.2.3.3 and 4.5, respectively.

double check language used here in follow-up edit

However, there is a risk associated with better prediction after using optimization tools. The increase in performance from over-optimization could be linked to the training set performance and might not generalize outside of the specific type of input data used. A workaround for this scenario is to obtain more data for the set or to obtain a completely different data set altogether.

2.2.3.1 Training Set Size

The first diagnostic plot for optimizing the model performance is called a *learning curve*, which provides information about the bias-variance tradeoff with respect to the data set size. More specifically, learning curves compare the training and cross-validation errors to the size of the training set (i.e.,

number of instances in the training set). This is done by randomly selecting a percentage of the the training set, inputting that into a statistical learner, and tabulating the error of the learned model.

Typically, a learning curve will look somewhat like one of the three examples in Figure 2.9[3]. A learning curve tests the model for high bias or high variance, which can correspond to an under- or overfit model, respectively.

Figure 2.9a suggests underfitting because the model is missing important features in the data. It is characterized by a small gap between the curves but high overall errors. The cross-validation error remains consistently high and the training error increases drastically with increasing data, since it is not generalizing well.

Figure 2.9c suggests overfitting because the model has too much sensitivity to variations in the data. It is characterized by a very large gap between the curves. It has an extremely low training error, as it has taken into account every detail of the training set, but a high cross-validation error because it cannot generalize beyond the testing set.

Figure 2.9b is an example of a more ideal model fit. It is characterized by a small gap between the two errors, and they are at a reasonable level with respect to the desired performance. The training error should increase with respect to the training set size due to a larger amount of bias (preventing overfitting). However, the cross-validation error should decrease quickly

[3]These schematics are based on hand-drawn diagrams by Ritchie Ng on http://www.ritchieng.com/applying-machine-learning/

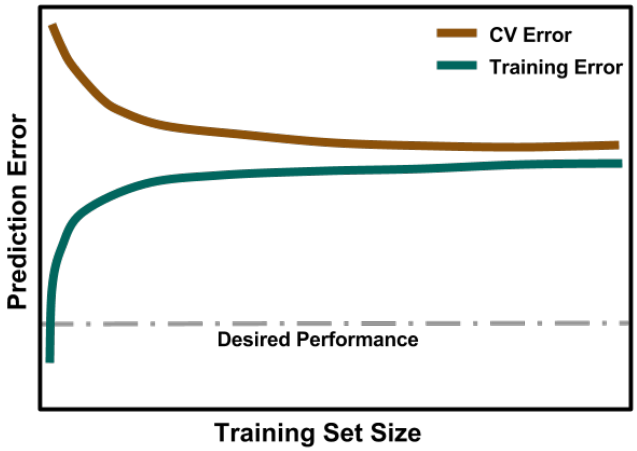

(a) High bias

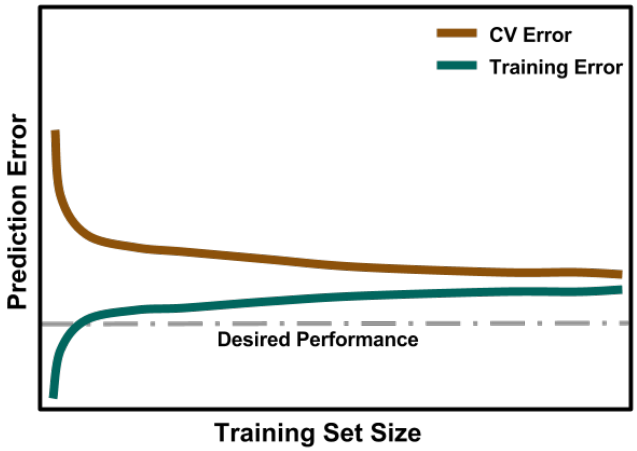

(b) Ideal

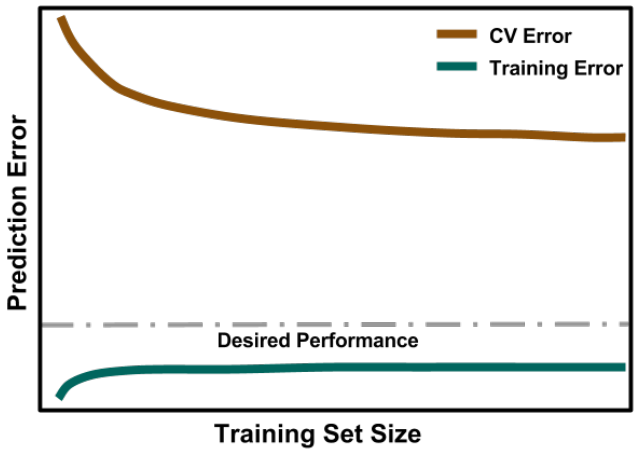

(c) High variance

Figure 2.9: Learning Curves for Three Training Scenarios

with respect to the training set size due to being close to the minimum of the bias-variance tradeoff.

The training set size must be large and diverse enough to be considered independent and identically distributed (i.i.d.) because most ML algorithms are developed upon this assumption. Sometimes this is not possible, and the training data are skewed, i.e., a portion of the data is over-represented. This must be handled explicitly, but only involves simple parameter changes in scikit-learn [24]. Each algorithm handles skewed data differently, so it is beyond the scope of this work.

2.2.3.2 Model Complexity

After ensuring the appropriate training set size is selected, the models must be further optimized using *validation curves*. These provide information on the bias-variance tradeoff with respect to model complexity. Two main tuneable factors affecting model complexity can cause the model to be under- or overfit to the data: number of features in the data set and algorithm parameters that control the regularization.

Figure 2.10 adapted from Ref. [6] shows the optimum as the minimum of the cross-validation error curve in the main (bottom) plot. There is some gap between it and the training error, much larger than the left side of the plot and much smaller than the right. The top-middle plot is a simplified visualization of an approximately well-fit model. The left region is marked by both errors being quite high, and above is an illustration of how an

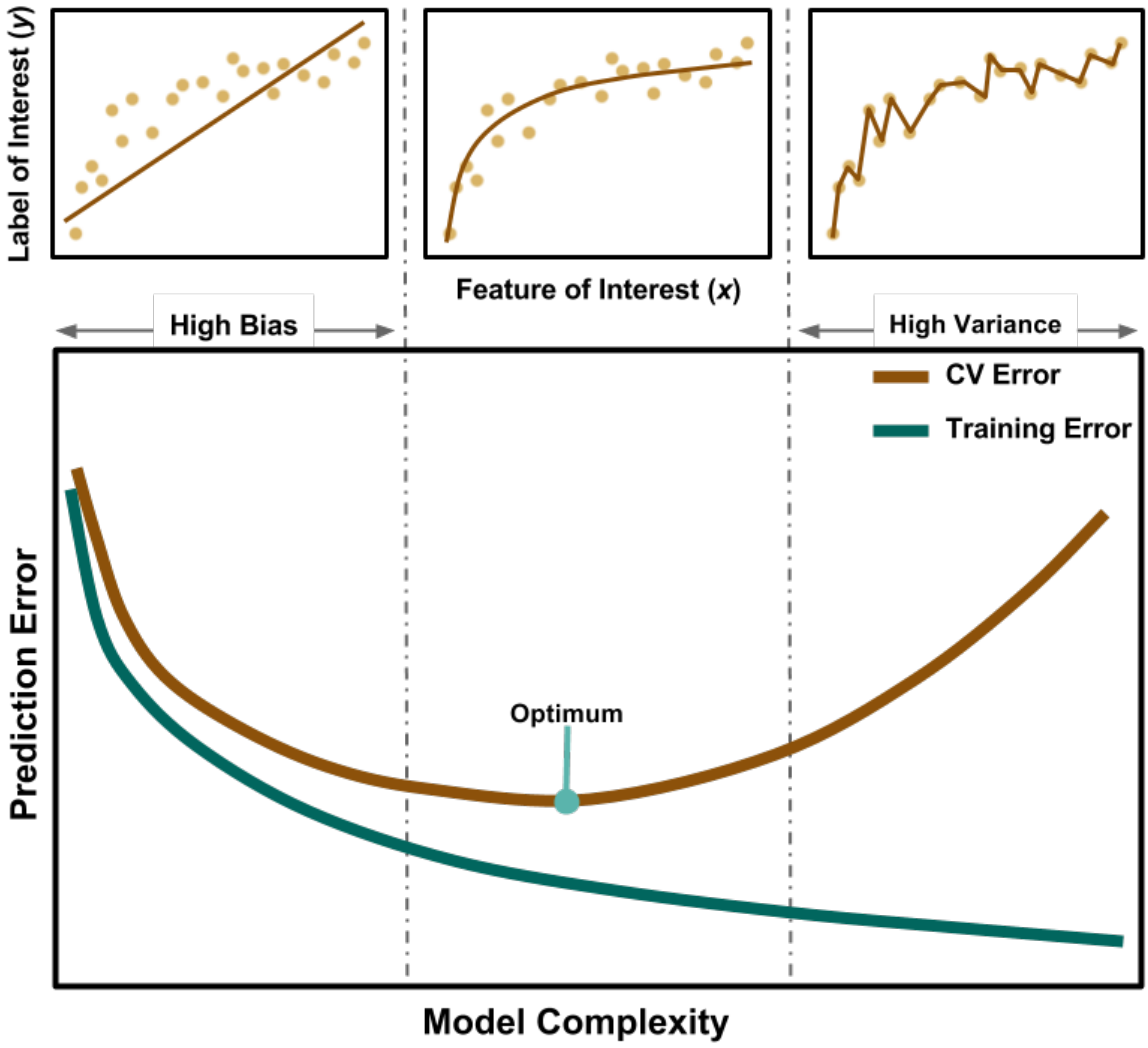

Figure 2.10: Validation Curve with Different Model Fits

underfit plot (high bias) could provide high errors. The right region shows the training error being quite low but the cross-validation error being high. The diagram differing options with how to adjust to skewed training sets [24]. above shows that it is obvious how the training error would be negligible,

but generalizing beyond that probably will not yield accurate results.

In practice, plotting learning and validation curves can be iterative. But as previously mentioned, too many optimizations will result in a poorly performing model when exposed to data outside of the training set.

2.2.3.3 Comparison of Models

In addition to evaluating a single learned model, it is beneficial to compare models. Moreover, there are potential degeneracies in the solution space. This is because most inverse problems are *ill-posed*, because the solution is not guaranteed to be unique [28]. Evaluating not only the solution, but the confidence in the solution, is therefore prudent.

Both solution uncertainty and model comparison can be done using Bayesian inference as discussed in Section 2.1.2. Equations 2.1 and 2.2 show that there are three values to obtain to calculate a posterior probability, i.e., the probability of a parameter estimated from an ML model being correct: likelihood, prior probability, and marginal likelihood. Comparing posterior probabilities among different models reveal the most probable correct answer, i.e., the highest posterior probability. [29, 30] Each of these values are explained futher below.

The posterior probability represents the solution to an *inverse* problem, where model parameters are predicted from some given measurement values. It is not directly computable and thus the remaining probabilities discussed below indirectly allow its computation. In this context, it is the probability

that a predicted reactor parameter from a chosen ML algorithm is correct given input based on an SNF recipe. For example, it is the probability that a plutonium-239 concentration of $y\%$ is attributed to a uranium oxide fuel in a boiling water reactor (BWR) with a burnup of $x\ GWd/MTU$.

The prior probability represents the solution to a *forward* problem, where measurement values are predicted from some given model parameters. In this context, this is calculated from the instances in the training data set. The likelihood is the probability that the output SNF composition of a simulation is correct given the input of reactor operation parameters. In practice, it will be calculated from a large number of forward simulations using ORIGEN, i.e., the training data set. For example, this would be the probability that uranium oxide fuel from a BWR having a burnup of $x\ GWd/MTU$ contains $y\%$ of plutonium-239.

The likelihood represents the spread of plausible *model parameters*, so it is a hypothesis based on the breadth of the model space with no evidence provided. In other words, it is given by model parametertization from a number of potential sources. One method is expert-elicited values. Another is a predicted model from some established theory or previously known relationship, e.g., empirical relations between isotopic ratios and certain reactor parameters or a direct calculation of the reactor parameters. In this context, it is obtained from the estimated model parameters from a given statistical model. For example, it is the probability that a model from SVR predicts a burnup of $x\ GWd/MTU$ for uranium oxide fuel from a BWR

with no other direct measurements provided.

The marginal likelihood represents the spread of plausible *measurements*, so it is based on the breath of the data space with no model-based information provided. In practice, however, it is calculated by summing the joint probabilities of all possible model parameter hypotheses and measurements. This in essence provides a normalization constant for the Bayes' equation. Thus, the marginal likelihood is only needed for absolute posterior probability calculations; it does not affect the relative probabilities, which are all that is needed for model comparison. [30, 31]

For reference, Table 2.1 is a summary of the Bayes' theorem components described above as related to this work. In the table, **P** is a probability, **D** is a set of measurements (i.e., data), and **M** is a set of model parameters. The examples used in the discussion above are reiterated here.

2.3 Computational Methods

There can be a large number of computational tools within a given field of study. They are typically developed with a single aspect of analysis in mind, so one must understand the simplifying assumptions the developers made for their purposes. Thus, choosing a computational tool is not always obvious. This section both introduces and defends the choices for the various experimental components.

Probabilities	Calculation Method and Example
P(D|M) Prior	*Given:* M = BWR U-oxide with burnup = ***x*** GWd/MTU *This is true:* D = nuclide vector with Pu-239 = ***y***% *With:* ***z***% probability *Calc'd from:* ORIGEN simulations in training set
P(M) Likelihood	*Given:* No direct information on D *This is true:* M = BWR U-oxide with burnup = ***x*** GWd/MTU *With:* ***z***% probability *Calc'd from:* Machine-learned model prediction
P(D) Marginal L.	*Given:* No direct information on M *This is true:* D = nuclide vector with Pu-239 = ***y***% *With:* ***z***% probability *Calc'd from:* Summation of training set instances
P(M|D) Posterior	*Given:* D = nuclide vector with Pu-239 = ***y***% *This is true:* M = BWR U-Ox with burnup = ***x*** GWd/MTU *With:* ***z***% probability *Calc'd from:* All quantities above

Table 2.1: Summary of Bayes Theorem Components

2.3.1 Fuel Cycle Simulation

Nuclear fuel cycle studies involve tracking the material flow of nuclear fuel. This can be anywhere from mining to waste management, or focus on a process step in between. Fuel cycle studies are not necessarily nuclear-specific. For example, they can be used to evaluate economic predictions, environmental impact, transportation planning, etc. In order to draw conclusions from these studies, it is common to use a nuclear fuel cycle simulator that tracks the quantities of interest. These allow the comparison of different fuel types, reactor technologies, material processing steps, etc.

There are simplifications researchers need to make in order to experiment in a controlled way. Fuel cycle simulators, built for a specific needs, must remove complicating factors that are less relevant to the study. For example, one tool might be suited well to large-scale systems analysis with little nuclear physics included in the models, and another might focus on detailed isotopics within a system to track plutonium.

Because a large portion of a nuclear forensics investigation relies on measuring isotopics, ORIGEN [25] within the SCALE code system was chosen for its physically detailed models of activation, depletion, and decay. ORIGEN is a part of the SCALE 6.2 modeling and simulation suite of computational tools developed for nuclear design and safety [23]. Specifically, the ARP module of the code was used: ORIGEN-Automatic Rapid Processing (ORIGEN-ARP).

ORIGEN calculates time-dependent nuclide concentrations (or quantities

derived from these) that result from activation and depletion calculations. The physics (i.e., neutron transport and decay) calculations are carried out in other SCALE modules that solve the depletion equations. This generates libraries for ORIGEN that include the probabilities of reaction (i.e., cross sections) for the system.

To obtain an SNF recipe from a reactor simulation, ORIGEN uses the desired input power generation with the cross section library to calculate a flux, the resulting depletion, and the end composition (i.e., isotopic recipes or nuclide vectors). Another output is decay; the composition is computed using decay equations with nuclear data [2]. These compositions provide source terms for other calculations, such as decay emission spectra from neutrons, alpha particles, beta particles, and gamma rays. Other derived quantities like activity, decay heat, or radiological hazard factors are also an option.

ORIGEN-ARP allows users to access a wider range of simulations by interpolating between the pre-calculated libraries instead of creating new libraries. It is known to be validated for light water reactor (LWR) SNF [15]. Additionally, recycled SNF in the form of mixed oxide fuel has been benchmarked for the relevant reactors [4]. Through ORIGEN, given an initial material composition, some reactor operation parameters, and a reactor type, one can quickly perform many different nuclear reactor simulations and obtain SNF recipes.

2.3.2 Statistics Toolkit

The statistics toolkit chosen for this work is scikit-learn [24], a machine learning package in python. Virtually all modern ML toolkits will have acceptably fast and reliable algorithms, but the use of python provides a platform for seamless integration of all the tools in the workflow.

2.3.3 Computational Gamma Spectra

Although the data modification shown later in Section 3.1.2 does not use any standalone tool, the code GAmma Detector Response and Analysis Software (GADRAS) [7] developed at Sandia National Laboratories will provide information reduction in a physically valid manner. Test studies will be carried out using the gamma energies available from ORIGEN simulations, but the detector response will need to be varied more than this tool can provide. Thus, given the gamma energies from ORIGEN and a user-chosen detector response function (DRF), GADRAS computationally generates gamma spectra. This will enable a more robust study of statistical performance with respect to information reduction.

2.4 Applications of Statistical Methods to Nuclear Forensics Analysis

Although the body of literature on the area of proposed research is not expansive, there have been a number of relevant studies on the prediction of forensically relevant categories or quantities of nuclear materials using statistical methods.

2.4.1 Special Nuclear Materials Studied

With regards to broader forensics capabilities, materials from different steps of the nuclear fuel cycle are being studied. Even though each material has its own forensics signatures, the process of applying statistical methods to the analysis of material provenance is similar for each.

For example, on the front end of the fuel cycle, an entity may have obtained UOC if they have enrichment capabilities. One study performed statistical analyses on UOC from 21 sources (throughout seven countries) using 30 concentration measurements of various elements, isotopes, and compounds, e.g., sodium, magnesium, thorium, uranium-234, or halide compounds [27]. The goal of classifying the source and the country was reached 60% and 85% of the time, respectively.

On the back end, an organization might have interest in SNF if they have reprocessing capabilities. Or, perhaps already separated plutonium from SNF has been intercepted and needs to be traced. Another study addresses

this by performing factor analysis on theoretical separated plutonium from various sources of ORIGEN-simulated SNF based on their composition at the end of irradiation [20]. Since in this study all materials are the same age, five plutonium isotopes ($A = 238 - 242$) correctly predicted a test sample. However, taking different times since irradiation and reprocessing into account requires more isotopic measurements.

2.4.2 Statistical Methods Employed

There are statistical methods studies that focus on the classification of the reactor type for unknown samples [10, 20, 21, 27]. However, this work is focused on burnup prediction. Although the results for both regression and classification are based on a number of features that are usually isotopic in nature, it is not clear if the regression counterparts of these algorithms will perform similarly for this task.

Promising regression work using factor analysis has been published [19, 22]. Although factor analysis explicitly requires the input of domain knowledge, it is a valuable first step towards understanding how statistical methods can provide insightful models that predict fuel enrichment and burnup. In the following two cases, the features included for the analysis are only the uranium and plutonium isotopes remaining in the SNF. Ref. [19] covers predicting enrichment and burnup from a range of simulated SNF recipes and comparing an 'unknown' sample to the results of the factor analysis. Ref. [22] extends that study to real measured samples from the

spent fuel isotopic composition (SFCOMPO) database [17]. This work also highlights and addresses a known problem: reliable discrimination between SNF from pressurized water reactors (PWRs) and boiling water reactors (BWRs).

The most closely related work to this study involves not only statistical methods but an investigation of those methods when faced with information reduction via random nuclide measurement errors in the training data set [3]. Additionally, feature reduction was investigated by using various nuclide compositions: the top 200 nuclides by concentration in each vector, fission products only, and a PCA-derived shortened nuclide list. Three methods were compared. First and second, the nearest neighbor algorithm using both L_1 (sum of absolute differences of Cartesian coordinates) and L_2 norms for measuring distance between test data points classified reactor type and predicted burnup. Third, ridge regression with an L_2 norm for regularization was only applied to burnup prediction. In both classification and regression cases, using the fission products nuclide list with both nearest neighbor methods performed the best. All other nuclide lists quickly devolved to random guesses with an increase in nuclide error in the case of reactor prediction, and more than 100% error in the case of burnup prediction.

For reliable prediction, it seems to be promising to use actinides [19, 22] and/or fission products [3] for domain knowledge-based feature reduction. However, this work intends to still investigate statistical methods for dimensionality reduction, e.g., PCA. This could be beneficial in prediction of

burnup or other reactor parameters, or could be useful in other ways, such as visualization or discovering new correlations among SNF properties as new reactor technologies are deployed.

3 METHODOLOGY AND DEMONSTRATION

This chapter first covers the methodology of the proposed work by introducing each experimental component and following up with a demonstration of each component. This has been split into three sections, summarized below.

Section 3.1 discusses how the training data set is obtained. This is a set of observations with known inputs, i.e., labels that are to be predicted. After the initial training data is simulated in Section 3.1.1, with a possible information reduction step in Section 3.1.2, the data set will be input to a statistical learner for the next step: training a model.

Section 3.2 is about which algorithms use the training set. They use the features and labels in the training data to formulate a model. Algorithm choice and parameters are discussed in Section 3.2.1. Next, the main goal for these ML models is to supply reactor parameters associated with some unknown SNF. Section 3.2.2 shows the results of testing this goal: the prediction of a new instance that has only features and no burnup label.

Finally, the algorithms are evaluated for accuracy and validated, as shown in Section 3.3. In practice, validation implies more than just ensuring the models are properly fit to the data. Perhaps the training set was not representative of the actual data space, whereas non-statistical methods do not rely on the data space for results. To both understand the performance of the models, the results are then evaluated for over- or under-fitting.

The demonstrations of the above are based on previous work on the

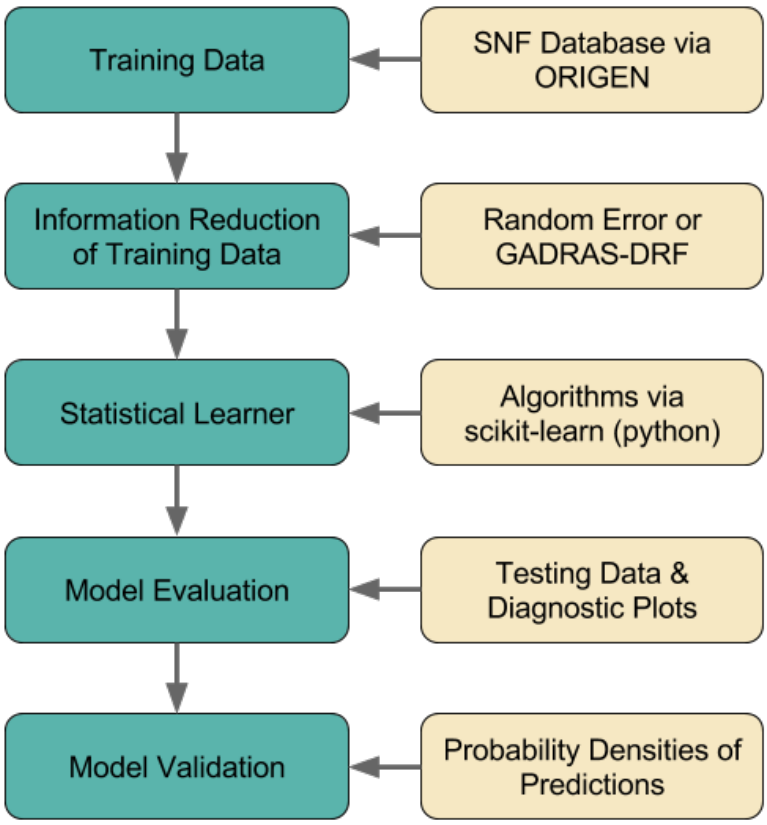

Figure 3.1: Methodology of Proposed Experiment

subject [3] regarding ML model performance with respect to information reduction. Replicating the methodology helps to establish some baseline expectations of reactor parameter prediction and how the different algorithms perform.

Next, this work will expand upon the previous work. The first is adding a different information reduction technique via using gamma energies from the SNF nuclide recipes. Following this, one could apply a DRF that

calculates various spectra based on the types of gamma detectors available to the forensics community (This particular information reduction step is not demonstrated here). Secondly, a more advanced ML algorithm, support vector regression, is included to compare a complex model against the two simpler models. A schematic of the workflow involving the experimental components is shown in Figure 3.1.

3.1 Training Data

3.1.1 Spent Nuclear Fuel Simulations

Because creating databases from real measurements to represent reactor technologies from around the world is impossible, the database in this study is created from high-fidelity simulations via ORIGEN [25]. A set of simulations of SNF at different burnups and cooling times comprises the database. Of interest to an entity trying to create a weapon is partially irradiated fuel if they have plutonium separations capabilities or any radioactive substance in the case of a dirty bomb. Addressing the former, a smaller burnup than is typical for SNF from a commercial reactor is used in the previous work. This will be repeated here for demonstrative purposes, but expanded upon in future work.

As mentioned in Section 2.2.3, many algorithms are developed on the assumption that the training set will be independent and identically distributed (i.i.d.). This is important so that the model does not overvalue

ORIGEN Rxtr	Rxtr Type	Enrichment
CE14x14	PWR	2.8
CE16x16	PWR	2.8
W14x14	PWR	2.8
W15x15	PWR	2.8
W17x17	PWR	2.8
S14x14	PWR	2.8
VVER440	PWR	3.60
VVER440_3.82	PWR	3.82
VVER440_4.25	PWR	4.25
VVER440_4.38	PWR	4.38
VVER1000	PWR	2.8
GE7x7-0	BWR	2.9
GE8x8-1	BWR	2.9
GE9x9-2	BWR	2.9
GE10x10-8	BWR	2.9
Abb8x8-1	BWR	2.9
Atrium9x9-9	BWR	2.9
SVEA64-1	BWR	2.9
SVEA100	BWR	2.9
CANDU28	PHWR	0.711
CANDU37	PHWR	0.711

(a) Reactor types and uranium-235 enrichment [weight%]

	PWR	BWR	PHWR
Power Density [MW/MTU]	32	23	22
Burnup [MWd/MTU]	600–17700	600–12300	600–12300
Cooling Time		{1m, 7d, 30d, 1y}	

(b) Simulation space defining reactor parameters and cooling time

Table 3.1: Design of the Training Set Space

or overfit a certain area in the training space. As this is not easily proven, it requires extensive knowledge of worldwide commercial reactors. Most obviously, a truly i.i.d. training set would go beyond the lower burnups, but this is purely for demonstration with a single use case in mind.

The training database is thus constructed by simulating the same training set space as described in Ref. [3], shown in Table 3.1. For each entry shown here the simulations included the span of cooling times and burnups in Table 3.1b. The power densities, listed enrichments, and moderator densities were kept constant. The burnup for the PWRs was increased in steps of 950 MWd/MTU, resulting in 19 measured time points. The BWRs and pressurized heavy water reactors (PHWRs) had 18 measurements with burnup steps of 690 MWd/MTU. This resulted in 2313 observations in the training set.

Feature reduction on the training set is manual in nature: the top 200 nuclides by concentration in each observation were retained. Other reduction techniques using domain knowledge (e.g., filtering for actinides) and statistical dimensionality reduction (e.g., PCA) are not addressed in this demonstration.

While typical ML studies choose the testing set randomly from the training set, the previous work used an external one, shown in Table 3.2. The simulations retained the default values from the training set; only the values shown here were changed. This provided 92 observations for testing. The test set was designed to have values in between the trained

Fuel	Reactor	Enrichment	Cooling Time	Burnup
CANDU28	PHWR	0.711	{1m, 7d, 30d, 1y}	{1400, 5000, 11000}
CANDU28	PHWR	0.711	{3m, 9d, 2y}	{5000, 6120}
CE16x16	PWR	2.8	{1m, 7d, 30d, 1y}	{1700, 8700, 17000}
CE16x16	PWR	2.8	{3m, 9d, 2y}	{8700, 9150}
CE16x16	PWR	3.1	{7d, 9d}	{8700, 9150}
GE7x7-0	BWR	2.9	{1m, 7d, 30d, 1y}	{2000, 7200, 10800}
GE7x7-0	BWR	2.9	{3m, 9d, 2y}	{7200, 8800}
GE7x7-0	BWR	3.2	{7d, 9d}	{7200, 8800}

Table 3.2: Design of the Testing Set Space

values of burnup and cooling times for the same set of reactors. However, a systematically chosen test set can be problematic since it may not cover parts of the training space. It is implemented in this study for comparison, but cross-validation will be used moving forward. More specifically, using k-fold cross-validation is expected to better indicate the model performance.

3.1.2 Information Reduction

Since the overall goal of this project is to determine how much information to what quality is needed to train an ML model, there will be an information reduction manipulation applied to the training data set. This study evaluates the impact of randomly introduced error on the ability of the algorithms to correctly predict the burnup.

The three algorithms will be evaluated with error applied to each nuclide vector in the training set. A maximum error ranging from $0 - 10\%$ is

chosen for each round of training, and a random error within the range of $[1 - E_{max}, 1 + E_{max}]$ is applied to each component of the nuclide vector.

However, error in a nuclide vector is not random, in fact it is systematic and dependent on a number of known sources of uncertainty. The next study will introduce error by limiting the nuclides to only those that can be measured with a gamma spectrometer. Although this is initially done using the availability of gamma energies in ORIGEN, GADRAS can provide more DRFs to further reduce information given to the algorithm.

3.2 Statistical Learning for Models

3.2.1 Algorithms Chosen

Choosing which algorithms to test is largely intuitive. It is based on the strengths and weaknesses of different optimization methods within the algorithms as well as what is being predicted.

For a benchmarking excercise, some ML approaches here were chosen based on previous work [3]: nearest neighbor and ridge regression. These are useful because they are simple, providing distance-based and linear-based models, respectively. If more complex algorithms are not required to obtain useful results, then there is no need to use more computationally expensive options. However, hedging on the fact that more complex models will be needed, this work also employs an algorithm that is known to handle highly dimensional data sets well: support vector regression. These algorithms

were introduced in Section 2.2.1.

Algorithm	Parameter	Value
Nearest Neighbor Regression	*n*-neighbors	1
	Weights	uniform
	Distance Metric	L2: Euclidian Distance
Ridge Regression	Regularization, α	1.0
	Normalization	False
	Stopping Tolerance	0.001
Support Vector Regression	Kernel	Radial Basis Function
	Gamma, γ	0.1
	C	1.0
	Epsilon, ε	0.1
	Stopping Tolerance	0.001

Table 3.3: Algorithm Parameters Used in Demonstration

The parameters chosen for the algorithms are shown in Table 3.3. For many, the default behavior was retained. Prior to training, the data set is preprocessed by scaling and normalization because the nuclide concentrations vary by many orders of magnitude. Algorithm implementations from a python-based ML toolkit, scikit-learn [24], are used to train the models.

3.2.2 Reactor Parameter Prediction

The above was carried out, training various statistical models of SNF using nuclide correlations with burnup. As a reminder, this is not the entirety of the

nuclode output from ORIGEN; it is the top 200 nuclides by concentration in each row. Following the training phase, it is important to estimate the reactor parameter prediction capabilities of those models by testing their generalizability. This is done with the previously described set of measurements from a test data set (shown in Table 3.2) with samples that mimic potential interdicted SNF. The testing set has the same features as the training set, with known burnup labels that are compared to the predicted labels.

Figure 3.2: Prediction Error from Information Reduction via Random Error

Next, information reduction was carried out with all three ML approaches. Figure 3.2 shows the three algorithms' mean absolute percentage errors (MAPEs) with respect to the reduction of information by the introduction

of random error to the nuclide vectors, as described in Section 3.1.2. SVR is shown to perform the best, but it quickly reaches 100% error. Although ridge regression rapidly increases with any amount of error, nearest neighbor regression shows more promise, although it reaches 257% at 10% error. Overall, this performance indicates that these algorithms are unlikely to predict burnup when faced with the uncertainties in real-world measurements or the further reduction in information from gamma detection.

Discuss mape or change error here?

Algorithm	Error Origin	MAPE	RMSE [MWd/MTU]
Nearest Neighbor Regression	Testing Set	78.24	3479.0
	5-fold Cross-Validation	127.84	4401.4
Ridge Regression	Testing Set	0.44	44.96
	5-fold Cross-Validation	0.05	3.24
Support Vector Regression	Testing Set	4.32	428.52
	5-fold Cross-Validation	0.49	163.61

Table 3.4: Three Models' Burnup Prediction Errors

For no introduced error, each model's prediction errors are shown in Table 3.4. First, shown here are two *sources* of error: from the testing set and via cross-validation. Although previous work uses the former, it is expected that the latter will provide better estimates of model behavior. The models evaluated by the testing set do not have a validation set for pre-evaluation. The models that are evaluated via cross-validation do not use the testing set.

Table 3.4 also includes two error *metrics*. For the sake of comparison to

previous work and convenient interpretation, MAPE is tracked. However, MAPE is not the only error metric. Being that it approaches infinity near true values of zero, absolute and squared deviations can also be tracked and may provide more information. Anecdotally, the preferred method in the community is to use root-mean-squared error (RMSE) for model error estimation, so both are tabulated. Regardless, the MAPE shows that there are some extremely high and extremely low errors depending on the algorithm; both results indicate poor performance. This is quite concerning, because these results are from error-free data.

Despite this poor initial performance, the results in Table 3.4 and Figure 3.2 can be evaluated. Next introduced are some diagnostic and optimization procedures that can shed light on these results.

3.3 Validation

To obtain reliable models, one must both choose or create a training set carefully and study the impact of various algorithm parameters on the error. Although the title of this section suggests final steps of confirming a model's usefulness for predictions, what follows is more of a diagnostic exercise. In practice, these analyses can be used for both purposes.

ML algorithms are heavily dependent on the training inputs and algorithm parameters given to them, such as training set sizes, regularization, number of features in the training set, optimization parameters, etc. From

the results shown in Section 3.2, it is clear there is room for improvement. To evaluate these input and parameter variations, diagnostic plots show the errors between the predicted burnup values and the actual burnup values with respect to some variable on the x-axis. As previously introduced in Section 2.2.3, the prediction errors are compared to the training error to understand the generalization strength. These two errors are plotted with respect to training set size (learning curves) and the algorithm parameters governing model complexity (validation curves) to provide insight into the model fitness.

In addition to ML best practices, another layer of comparison is added here. Because it is difficult to ensure consistently representative testing data, the accuracy of a learned model should not depend on only one testing set. The learned model's accuracy is better estimated by using a validation set. Here, this is implemented as k-fold cross-validation, introduced in Section 2.2.2. This work includes both the testing error (using the testing set described in Section 3.1) and 5-fold cross-validation error. The predetermined testing set will allow for comparison against the previous work it was obtained from [3], but it is assumed that cross-validation will provide a better indication of model performance because the entirety of the training set has also been tested.

The learning curves are obtained as follows, shown in Figure 3.3. For a given (randomly chosen) training set size between 15 and 100% of the

add other plots and describe

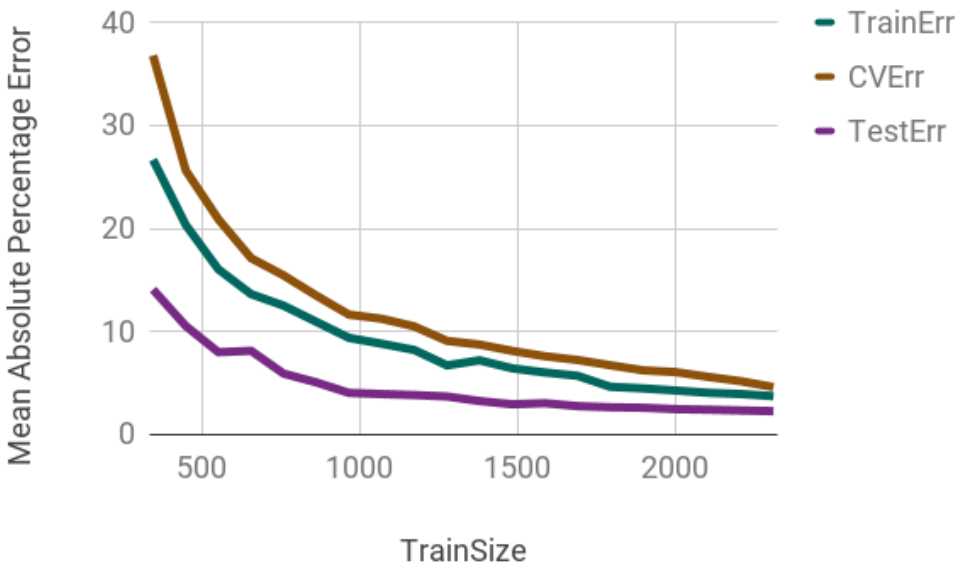

Figure 3.3: SVR Learning curve for burnup prediction, $\gamma = 0.001$

total data set, training and prediction rounds were performed for each. The testing error scenario performs this $n = 5$ times and averages those results. This is chosen to be equivalent to the k in k-fold cross-validation to ensure comparable statistics. The cross-validation error scenario has no need for averaging because it is performed automatically. The learning curve plot does not provide a clear picture of over- or undertraining upon first glance.

expand on why

The validation curves are obtained as follows, shown in Figure 3.4. The γ parameter in SVR, which influences model complexity, was varied from 10^{-4} to 10^{-1}. Note that in Figure 3.4 the domain has been decreased to show the features close to the y-axis. Training and prediction rounds were performed for different γ values in this range. Again, the testing and cross-validation

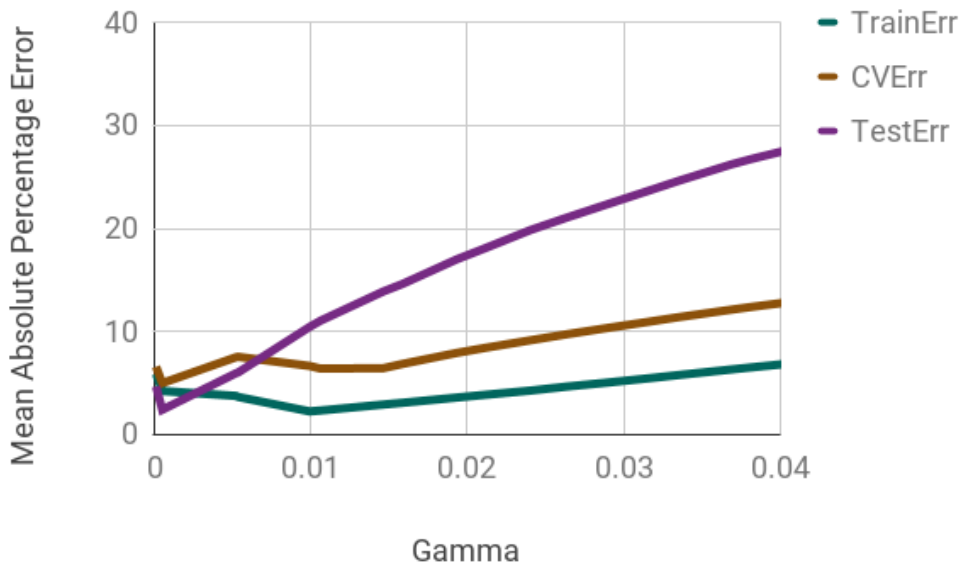

Figure 3.4: SVR Validation Curve for Burnup Prediction, $TrainSize = 2313$

errors are both used as described above. As with Figure 3.3, determining the robustness to over- or undertraining is difficult here although there is possibly a minimum at $\gamma = 0.001$.

Although there is no example behavior of Figure 3.3's peculiar learning curve in Figure 2.9, the curves mimic the squared bias curve from Figure 2.7. This suggests that the bias in the model is much higher than the variance. Next, the testing error is lower than the training error; this should never be the case, and indicates an issue with the systematically chosen testing set. While the cross-validation error is correctly higher than the training error, it follows along in parallel, producing no information on model fitness other than confirming a very high bias. It is presumed this is not the fault

add other two plots of nn and rr; also add in C plots too

determine if c and gamma have any

of the algorithms, but the training set itself. It is likely covering too small of a range of the simulation space.

Additionally, Figure 3.4's validation curve shows the testing error dropping below the training error for extremely small γ, around where a minimum might be. Since the model suffers from high bias, no amount of model complexity can be optimized. The resolution to the underfitting is discussed in Section 4.1.

4 RESEARCH PROPOSAL

This document previously demonstrated the performance of ML on a set of nuclear material isotopics to calculate a reactor parameter of interest: burnup. Additionally, the procedures for understanding the learned model's behavior and thus the quality of the results was discussed. Next, a set of experiments are presented here.

Before describing the experiments, some preporatory topics and issues are addressed in Section 4.1. Next, the proposed research experimental design is presented. Sections 4.2, 4.3, and 4.4 describe evaluating the viability of statistical learning using direct isotopic information, information obtained from gamma spectra, and other fuel cycle flows, respectively. Discussed separately is the planned implementation of comparing methods using the Bayesian framework in Section 4.5. Finally, the timeline of this project is covered in Section 4.6.

4.1 Experiment Preparations

Expanding Training Set

As identified in Section 3.3, the testing set used for the demonstration was not suitable for further study without being expanded. Also mentioned was that many algorithms are developed on an assumption that the training set will be independent and identically distributed (i.i.d.). This is important so

that the model does not overvalue or overfit a certain area in the training space. The next step is to provide a larger, more diverse training set to the algorithms so they can better predict labels when faced with new instances. This diversity will be suggested from the SFCOMPO database [17], as it includes many common domestic and international reactors.

The SFCOMPO-2.0 relational database [17] has approximately 750 chemical assay measurements of SNF from 44 reactors. While this is not sufficient as a training set, it provides a better framework for a training set. It will be simulated with ORIGEN as inspired by the breadth of values in the SFCOMPO database. After cross-validation, diagnostics, and optimization, the ML models can be tested against the entries in this database to provide a clear estimate of of the model performance.

Finalizing Set of Algorithms

The three algorithms in the demonstration (nearest neighbor, ridge, and support vector regression) are not necessarily the set that will be evaluated for the experiments. After these are used to train new models on a larger training set for comparison, other algorithms can be speedily assessed as well. The scikit-learn toolkit allows for easy transitions because the algorithms are already implemented; applying a new ML algorithm involves merely changing the method. Since support vector-, distance-, and linear-based models are already represented, other obvious choices include Bayesian methods, decision trees, neural networks, or ensemble methods [6].

Computational Framework and Resources

Thus far, all simulations and training have not required more processing than available on a personal computer. However, some algorithms do require larger amounts of computational time (e.g., neural networks). If necessary, the training stage can be done using the Center for High Throughput Computing (CHTC), which is available to University of Wisconsin researchers.

4.2 Experiment 1

Viability of Statistical Learning on Direct Isotopics

The first experiment will be a purposefully constructed version of the demonstration: evaluating the model performance with known isotopics. This sheds light on how this methodology will perform on the simplest scenario, providing an upper estimate of performance. *The main purpose of this experiment is to probe the usefulness of statistical methods for determining reactor parameters, ultimately choosing the best performing methods.*

Figure 4.1 shows what type of input can be used for training and prediction. The two horizontal boxes are the physical and computational forms of what these experiments are simulating, respectively. The lab-measured mass spectra correspond to the perfect information being referred to here. In the computational context, these measurements instead come from simulations. Mass spectra results are thus approximated as the direct isotopics given from the simulations, since they provide highly reliable and accurate information.

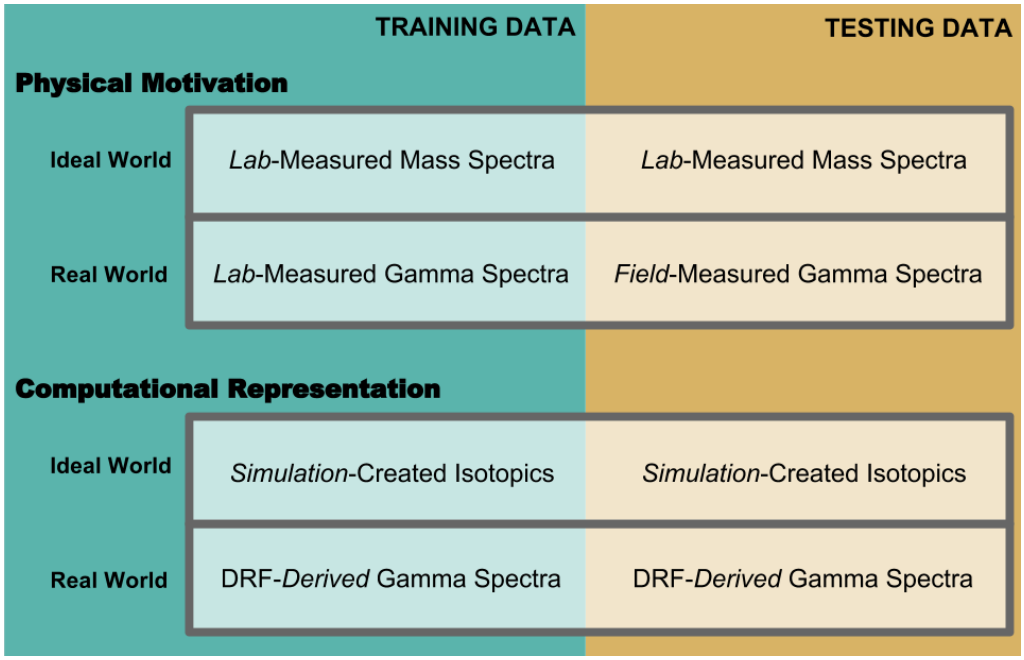

Figure 4.1: Motivation for Data Sets for Experiments 1 and 2

The variables for this experiment will include the following:

1. the complexity of the ML algorithm used,
2. feature reduction, and
3. different subsets of the decision space.

As previously mentioned, there are complexity differences among the algorithms, which will be taken into account. The distance-based nearest neighbor algorithm is by far the simplest, as it does not do any learning. By contrast, SVR with a radial basis function kernel to enable learning in higher orders is much more elaborate. The feature reduction will be different subsets of isotopes, e.g., top n nuclides by concentration, actinides only, fission products only, etc. Reducing the decision space can be done

by, e.g., simplifying the regression task by fixing the reactor type. It is expected that a more complex algorithm (e.g., SVR) will be needed, and that preprocessing and/or manual feature reduction will assist in creating higher quality models. Simplifying the decision space should always improve prediction, but it is not obvious how much it will impact burnup prediction specifically.

Risks

It is possible that statistical models trained on direct isotopic information do not perform well enough. Other than attempting different types of algorithms, the next tuning would occur by preprocessing the data further, statistically performing feature reduction via PCA. If this is not sufficient, SNF may have too many or too few correlated features to provide reliable models across the space of current reactor technologies. Since separated plutonium and UOC have been also studied using these techniques, these materials could provide an alternate route to pbtain useable learned models. Additionally, this methodology would also work if applied to post-detonation materials. There is work on creating standard materials to represent the "urban canyon". The noise from irradiated concrete, building materials, etc. is expected to pose a great challenge to forensics teams. This is another evolving subject that may benefit from statistical correlations [8].

4.3 Experiment 2

Viability of Statistical Learning on Gamma Spectra

The second experiment will be the previously discussed extension of the demonstration by applying DRFs to the gamma energies: evaluating the model performance with reduced isotopic information. This demonstrates the usefulness of this methodology in a real-world scenario where exact isotopics are not always known. *The main objective of this experiment is to measure the reduction in statistical model parameter prediction reliability as the quality of the training information is reduced.*

The two bottom portions of the boxes in Figure 4.1 represent a more realistic measurement scheme, involving a model trained from gamma spectrometers rather than the lengthy process of performing mass spectrometry on the samples. In the physical context, the measurements for training would be done using a semiconductor gamma detector, but the testing or prediction step may be done outside of the lab on a different detector. This will be captured by applying different DRFs to the radionuclide inventories from the simulations.

The variables for this experiment will include the following:

1. the complexity of the ML algorithm used,
2. feature reduction (implicit), and
3. quality of training and/or testing data set.

As in Section 4.2, performance will be explained with respect to algorithm

complexity. The feature reduction is implicit here, since gamma detection only includes radionuclides within the SNF isotopics. The indirect isotopic training data are likely going to reduce the prediction capability of the models, but it is not yet clear if a response function simulating a hand-held NaI gamma detector can provide any useful predictions. And while it is still expected that the complex algorithms will perform better, it is not yet obvious if different algorithms than the ones used in Experiment 1 will be needed.

Risks

Following the risks in Section 4.2,it is possible that statistical models trained on indirect isotopic information do not perform well enough. Different algorithms may perform better than others due to the underlying optimization processes. Further feature reduction could also prove useful, focusing on particular energy regions or particular peaks throughout the spectrum. The nature of the training information could be altered slightly by using an isotope identification algorithm; this may improve the performance, as the the typical field detectors are developed to automatically report isotopics from gamma spectra. If this still is not sufficient, it may be that direct isotopic information (i.e., that obtained from mass spectrometry) is required for reliable statistical models of SNF. Lastly, preprocessing could also be investigated here.

4.4 Experiment 3

Viability of Statistical Learning on Reprocessed Fuel

There is already nuclear fuel reprocessing in France for LWRs, and possibly in the forseeable future in China with fast breeder reactors. Given the existence of reprocessing in fuel cycles, it is important to develop nuclear forensics capabilities on processed SNF. This is presents an additional prediction challenge because many of the isotopic, chemical, and elemental signatures are stripped away in the processing. However, there is a possibility that plutonium isotopes can provide enough information for characterization, even with reprocessing [26]. Although Ref. [26] predicts reactor type and enrichment, it is enough motivation to pursue burnup as well.

This experiment is intended to repeat those in Sections 4.2 and 4.3 with an added layer of complexity from the reprocessing by including mixed-oxide fuel. It will be carried out using direct isotopics as in Section 4.2, with a goal to use indirect information as in Section 4.3 pending performance. The training data set will also be simulated using ORIGEN. *The main purpose of this experiment is to probe the difficulties of reactor parameter prediction when some of the inputs are from reprocessed nuclear fuel.*

The variables for this experiment will include the following:

1. the complexity of the ML algorithm used,
2. quality of training data set, and
3. type of preprocessing for feature reduction.

Because of the increased complexity of the training data, it is expected that a more involved algorithm will be necessary. The quality of the training data set will be varied as well as the type of preprocessing tool. It is not yet obvious if the feature reduction is absolutely necessary, but it is expected to improve the accuracy of burnup prediction. Feature reduction can be carried out via a range of discriminant, component, or factor analyses. Multiple studies have demonstrated success with some of these dimensionality reduction techniques [9, 10, 19, 21, 22, 26, 27]. Because reprocessing mixes streams of material, PCA is not expected to perform as well as ICA. This was discussed in Section 2.2.1.4.

Risks

It is possible that this framework is not the best approach to understand fuel cycles with reprocessing. The first action upon poor performance results is to try more/different preprocessing tools; this may have to include using domain knowledge to manually reduce the dimensions. As one of the goals within the nuclear forensics community is to identify new signatures and/or correlated measurements, this is not desireable but it could still offer interesting results. Also, some creativity could be applied to find a method that works for this type of dataset, such as the iterative partial least squares discriminant analysis used for determining UOC origin country and source prediction in Refs. [26, 27].

4.5 Method Comparison

It is essential to be able to compare the models proposed here against each other, but also against other analagous non-statistical methods. For example, Experiment 2 (Section 4.3) aims to predict reactor history values using simulated gamma spectra, and INDEPTH uses gamma energies/spectra as inputs. These can be directly compared using the inverse problem structure introduced in Section 2.1.2. An application of Equation 2.2 is discussed further in Section 2.2.3.3.

However, the Section 2.2.3.3 discussion excluded some detail for clarity. While initially uncertainties will be ignored for an approximate analysis, they cannot be ignored for long in the nuclear forensics context. These are quite important for obtaining some measure of confidence in the solution. Including the uncertainty broadens each predicted parameter to a range of probabilities. These are then analyzed to produce ranges of confidence in each prediction [31]. This means that the posterior probabilities discussed will not just be numbers, but probability distributions. The methods for calculating the necessary probability distributions are outlined below.

Here, we change the meaning of the variables to represent probability distributions, shown in Equation 4.1. C is a constant given by the marginal likelihood, which can be ignored when calculating relative probabilities, and $\boldsymbol{d}$ and $\boldsymbol{m}$ represent the training data set and model parameters, respectively. Thus, $P(\boldsymbol{d}|\boldsymbol{m})$ is the likelihood distribution function, $P(\boldsymbol{m})$ is

the prior probability distribution, and $P(\boldsymbol{m}|\boldsymbol{d})$ is the posterior probability distribution.

$$P(\boldsymbol{m}|\boldsymbol{d}) = C \ * \ P(\boldsymbol{d}|\boldsymbol{m}) \ * \ P(\boldsymbol{m}) \tag{4.1}$$

Mathematically speaking, the distributions are obtained by integrating over the relevant probability densities. For example, the prior probability distribution can be calculated from Equation 4.2, where $\boldsymbol{m}$ is the range of predicted model parameters, i.e. burnup values, and $\boldsymbol{d}$ is a set of nuclide vectors. Also, here, $\rho(\boldsymbol{x}) = \prod_i \rho(x_i)$.

$$P(\boldsymbol{m}) = \int_{\boldsymbol{m}} \rho(\boldsymbol{d}) d\boldsymbol{d} \tag{4.2}$$

Similarly, the likelihood distribution function is obtained as in Equation 4.3.

$$P(\boldsymbol{d}|\boldsymbol{m}) = \int_{\boldsymbol{d},\boldsymbol{m}} \rho(\boldsymbol{d}|\boldsymbol{m}) d\boldsymbol{m} \tag{4.3}$$

In practice, however, these density functions are not calculated directly. Below, the methods chosen to estimate the functions in this work are addressed.

4.5.1 Estimating Density Functions

Estimating a probability density function $\rho(x)$ is not a straightforward task. One must have a sense for the shape of this function to predict a smooth curve that will represent the probability density over a range of a parameter. One estimation method is binning the parameters in the training set over

a given width and tallying up each bin to form a histogram; using some kernel, Gaussian for example, provides a function that should approximately follow the shape of the histogram. The shape of the histogram and function may strongly depend on the bin size, but this can be handled as a separate optimization step within the sci-kit learn package [24].

The prior probability distributions are given by the model space, e.g., reactor parameters as predicted from the ML models. The above-mentioned method should be utilized to obtain a prior density function from the range of burnups. This will not be necessary because the current design of the training set will provide a nearly flat density function (i.e., uniform distribution). However, this is not the case in a real-world scenario with mostly commercial reactor fuel comprising SNM inventories around the world. This topic will only be investigated if the training data set is changed. [31] Note: This implies the posterior is now only dependent on the likelihood.

The likelihood function can be obtained by summing the probability densities of each nuclide vector (d) given some predicted model parameter (m, e.g., a burnup prediction) using some algorithm (e.g., nearest neighbor regression). In essence, this is a large set of forward problems; it is information including the database of SNF recipes, and the known parameter inputs compared to the model's parameter predictions. The goal of this step is to find the *maximum* likelihood, usually carried out in a step called maximum likelihood estimation (MLE). In this framework, the training phase provides the maximum likelihood distribution through the use of cross-validation,

since the results are reported as a mean error with a standard deviation (which can be converted to accuracy for likelihood) [24].

Unfortunately, MLE is not this simple for other methods that do not employ cross-validation [29, 31]. This will indeed have to be broached in order to compare the machine-learned models against other forensics methods but has not yet been demonstrated (in progress).

4.5.2 Posterior Odds

Finally, a non-normalized posterior probability distribution, $P(m_i|d)$, can be calculated directly from the likelihood and prior distributions. The same can be done for a model obtained from a different algorithm, $P(m_j|d)$. The relative posterior probability distribution, aka *posterior odds* [31], can then be obtained as in Equation 4.4. Here, $B_{ij} = \frac{\rho(d|m_i)}{\rho(d|m_j)}$ and is referred to as the *Bayes factor*.

$$\frac{P(m_i|d)}{P(m_j|d)} = B_{ij}\frac{P(m_i)}{P(m_j)} \tag{4.4}$$

Given somewhat uniform priors, the Bayes factor is the key component that determines relative model performance. Table 4.1[1] shows an approximation of posterior probabilities calculated from $|lnB_{ij}|$. Taking the logarithm of the Bayes factor is done for convenience, since taking the product of many likelihoods tends towards zero.

In summary, given a mean-squared error and its standard deviation from

[1]This table is reproduced from Ref. [31].

$\lvert \ln B_{ij} \rvert$	Probability	Likelihood Strength
< 1.0	< 0.750	Inconclusive
1.0	0.750	Weak
2.5	0.923	Moderate
5.0	0.993	Strong

Table 4.1: Model Comparison using Likelihood Strength

using cross-validation with any ML algorithm, the MLE can be formed. To compare two models, a ratio of MLE_i to MLE_j, called the posterior odds, provides the probability of model i being correct.

4.6 Timeline

Figure 4.2 is an approximate timeline over which this work will occur. Multiple tasks will be complete before my internship is finished, and much of the computational framework is also complete. The experiments are expected to take a few weeks each, accounting for time spent on diagnostics and readying the results for the next step. Formal validation and model comparison will then be carried out. Because of reporting requirements, some preporatory writing will also be done during the internship. Thus, final analyses and writing are expected to take three months.

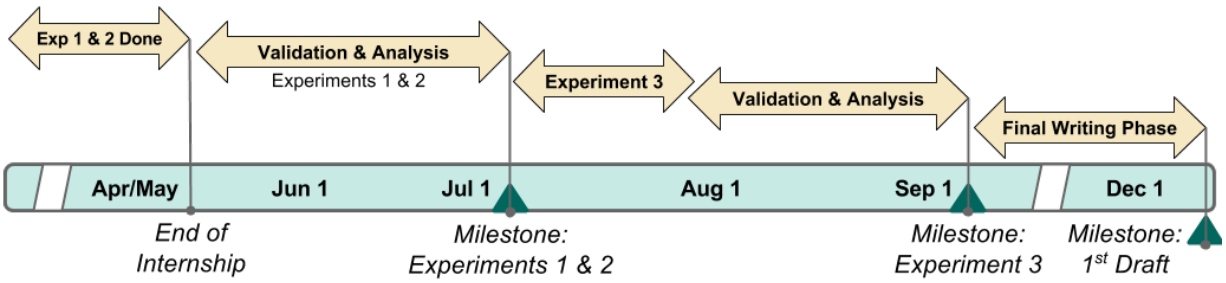

Figure 4.2: Timeline for Project

REFERENCES

[1] Broadhead, Bryan L, and Charles F Weber. 2010. Validation of inverse methods applied to forensic analysis of spent fuel. In *Proceedings of the Institute of Nuclear Materials Management 51st Annual Meeting*. Baltimore, MD, USA. https://www.osti.gov/scitech/biblio/1001291.

[2] Chadwick, M.B., M. Herman, P. ObloÅ¾inskÃ½, M.E. Dunn, Y. Danon, A.C. Kahler, D.L. Smith, B. Pritychenko, G. Arbanas, R. Arcilla, R. Brewer, D.A. Brown, R. Capote, A.D. Carlson, Y.S. Cho, H. Derrien, K. Guber, G.M. Hale, S. Hoblit, S. Holloway, T.D. Johnson, T. Kawano, B.C. Kiedrowski, H. Kim, S. Kunieda, N.M. Larson, L. Leal, J.P. Lestone, R.C. Little, E.A. McCutchan, R.E. MacFarlane, M. MacInnes, C.M. Mattoon, R.D. McKnight, S.F. Mughabghab, G.P.A. Nobre, G. Palmiotti, A. Palumbo, M.T. Pigni, V.G. Pronyaev, R.O. Sayer, A.A. Sonzogni, N.C. Summers, P. Talou, I.J. Thompson, A. Trkov, R.L. Vogt, S.C. van der Marck, A. Wallner, M.C. White, D. Wiarda, and P.G. Young. 2011. Endf/b-vii.1 nuclear data for science and technology: Cross sections, covariances, fission product yields and decay data. *Nuclear Data Sheets* 112(12):2887–2996. http://www.sciencedirect.com/science/article/pii/S009037521100113X.

[3] Dayman, Kenneth, and Steven Biegalski. 2013. Feasibility of fuel cycle characterization using multiple nuclide signatures. *Journal of*

Radioanalytical and Nuclear Chemistry 296:195–201. http://link.springer.com/article/10.1007%2Fs10967-012-1987-4.

[4] Gauld, I. C. 2003. Mox cross-section libraries for origen-arp. Tech. Rep., UT-Battelle, LLC and Oak Ridge National Laboratory. ORNL/TM-2003/2, https://www.nrc.gov/docs/ML0410/ML041040058.pdf.

[5] Gey, Frederic, Chloe Reynolds, Ray Larson, and Electra Sutton. 2012. Nuclear forensics: A scientific search problem. In *Proceedings of the Lernen, Wissen, Adaption (Learning, Knowledge, Adaptation) Conference*. Dortmund, Germany. http://metadata.berkeley.edu/nuclear-forensics/Paper_9-12-12_lwa-2012-nuclear-forensics-scientific-search-problem_v7.pdf.

[6] Hastie, Trevor, Robert Tibshirani, and Jerome Friedman. 2001. *The Elements of Statistical Learning*. Springer Series in Statistics, New York, NY, USA: Springer New York Inc.

[7] Horne, Steven M., Gregory G Thoreson, Lisa A. Theisen, Dean J. Mitchell, Lee Harding, and Wendy A. Amai. 2014. Gamma Detector Response and Analysis Software - Detector Response Function (GADRAS-DRF). User's Manual, Sandia National Laboratories, Albuquerque, New Mexico, USA. Version 18.5; SAND2014-19465, http://www.osti.gov/scitech/servlets/purl/1166695.

[8] Inn, Kenneth G.W., Jacqueline Mann, Jeffrey Leggitt, JoAnne Buscaglia, Simon Jerome, John Molloy, and William Pramenko. 2015. Nuclear forensic reference materials for attribution of urban nuclear terrorism. *Presentation for NIST*, https://www.nist.gov/sites/default/files/documents/oles/7-Inn_Kenneth-Nuclear-Forensics-UVC-Project.pdf.

[9] Jones, Andrew, Phillip Turner, Colin Zimmerman, and J.Y. Goulermas. 2014. Machine learning for classification and visualisation of radioactive substances for nuclear forensics. In *Techniques and Methods for Safeguards, Nonproliferation and Arms Control Verification Workshop*. Portland, Oregon. https://www.researchgate.net/publication/264352908_Machine_Learning_for_Classification_and_Visualisation_of_Radioactive_Substances_for_Nuclear_Forensics.

[10] Jones, Andrew E., Phillip Turner, Colin Zimmerman, and John Y. Goulermas. 2014. Classification of spent reactor fuel for nuclear forensics. *Analytical Chemistry* 86:5399–5405. http://pubs.acs.org/doi/ipdf/10.1021/ac5004757.

[11] Kristo, M.J., D.K. Smith, S. Niemeyer, G.D. Dudder, and R. Abedin-Zadeh. 2006. Nuclear Forensics Support: Technical Guidance Reference Manual. Tech. Rep., IAEA, Vienna, Austria. http://www-pub.iaea.org/MTCD/Publications/PDF/Pub1241_web.pdf.

[12] Langan, Roisin T., Richard K. Archibald, and Vincent E. Lamberti. 2016. Nuclear forensics analysis with missing data. *Journal of Radioanalytical and Nuclear Chemistry* 308:687. http://link.springer.com/article/10.1007/s10967-015-4458-x.

[13] Langley, Pat. 2011. The changing science of machine learning. *Machine Learning* 82:275–279. https://link.springer.com/article/10.1007%2Fs10994-011-5242-y.

[14] Lantzos, I., Ch Kouvalaki, and G. Nicolaou. 2015. Plutonium fingerprinting in nuclear forensics of spent nuclear fuel. *Progress in Nuclear Energy* 85(Supplement C):333–336. http://www.sciencedirect.com/science/article/pii/S0149197015300329.

[15] Leal, L. C., O. W. Hermann, S. M. Bowman, and C. V. Parks. 1998. Arp: Automatic rapid process for the generation of problem-dependent sas2h/origen-s cross-section libraries. Tech. Rep., Lockheed Martin Energy Research Corporation and Oak Ridge National Laboratory. ORNL/TM-13584, https://digital.library.unt.edu/ark:/67531/metadc684948/.

[16] May, Michael, Reza Abedin-Zadeh, Donald Barr, Albert Carnesale, Philip E. Coyle, Jay Davis, William Dorland, William Dunlop, Steve Fetter, Alexander Glaser, Ian D. Hutcheon, Francis Slakey, and Benn Tannenbaum. 2007. Nuclear Forensics: Role, State of the Art, and Program Needs. Tech. Rep., Joint Working Group

of the American Physical Society and the American Association for the Advancement of Science. https://www.aaas.org/report/nuclear-forensics-role-state-art-program-needs.

[17] Michel-Sendis, Franco, Jesus Martinez-GonzÃ¡lez, and Ian Gauld. 2017. Sfcompo 2.0 – a relational database of spent fuel isotopic measurements, reactor operational histories, and design data. *EPJ Web of Conferences* 146:06015. www.oecd-nea.org/sfcompo/.

[18] Moody, K.J., P.M. Grant, and I.D. Hutcheon. 2005. *Nuclear Forensic Analysis*. 1st ed. Boca Raton, Florida, USA: CRC Press. https://books.google.com/books?id=Q9mgDnWoPLYC.

[19] Nicolaou, G. 2006. Determination of the origin of unknown irradiated nuclear fuel. *Journal of Environmental Radioactivity* 86:313–318. http://nuclear.ee.duth.gr/upload/A13%20%20%20identification.pdf.

[20] ———. 2008. Provenance of unknown plutonium material. *Journal of Environmental Radioactivity* 99(10):1708–1710. http://www.sciencedirect.com/science/article/pii/S0265931X08000969.

[21] ———. 2009. Identification of unknown irradiated nuclear fuel through its fission product content. *Journal of Radioanalytical and Nuclear Chemistry* 279(2):503–508. http://link.springer.com./article/10.1007%2Fs10967-007-7300-x.

[22] ———. 2014. Discrimination of spent nuclear fuels in nuclear forensics through isotopic fingerprinting. *Annals of Nuclear Energy* 72:130–133. Technical Note, http://www.sciencedirect.com.ezproxy.library.wisc.edu/science/article/pii/S0306454914002308.

[23] Oak Ridge National Laboratory. 2016. SCALE: A Comprehensive Modeling and Simulation Suite for Nuclear Safety Analysis and Design. Code Suite, Oak Ridge National Laboratory, Oak Ridge, Tennessee, USA. Version 6.2.1, ORNL/TM-2005/39, Available from Radiation Safety Information Computational Center as CCC-834, http://scale.ornl.gov.

[24] Pedregosa, F., G. Varoquaux, A. Gramfort, V. Michel, B. Thirion, O. Grisel, M. Blondel, P. Prettenhofer, R. Weiss, V. Dubourg, J. Vanderplas, A. Passos, D. Cournapeau, M. Brucher, M. Perrot, and E. Duchesnay. 2011. Scikit-learn: Machine learning in Python. *Journal of Machine Learning Research* 12:2825–2830. http://scikit-learn.org/stable/index.html.

[25] Rearden, B.T., and M.A. Jessee. 2016. Ch. 5 Depletion, Activation, and Spent Fuel Source Terms. In *SCALE Code System: User Documentation*, 5–1–5–263. Oak Ridge, Tennessee, USA: Oak Ridge National Laboratory. Version 6.2.1; ORNL/TM-2005/39, https://www.ornl.gov/sites/default/files/SCALE%20Code%20System.pdf.

[26] Robel, Martin, and Michael J. Kristo. 2008. Discrimination of source reactor type by multivariate statistical analysis of uranium and plutonium isotopic concentrations in unknown irradiated nuclear fuel material. *Journal of Environmental Radioactivity* 99(11):1789–1797. http://www.sciencedirect.com/science/article/pii/S0265931X08001203.

[27] Robel, Martin, Michael J. Kristo, and Martin A. Heller. 2009. Nuclear forensic inferences using iterative multidimensional statistics. In *Proceedings of the Institute of Nuclear Materials Management 50th Annual Meeting*. Tuscon, AZ, USA: Institute of Nuclear Materials Management. LLNL-CONF-414001, https://e-reports-ext.llnl.gov/pdf/374432.pdf.

[28] Skutnik, Steven E., and David R. Davis. 2016. Characterization of the non-uniqueness of used nuclear fuel burnup signatures through a Mesh-Adaptive Direct Search. *Nuclear Instruments and Methods in Physics Research Section A: Accelerators, Spectrometers, Detectors and Associated Equipment* 817:7–18. http://www.sciencedirect.com/science/article/pii/S0168900216001571?via%3Dihub.

[29] Tan Bui-Thanh. 2012. A Gentle Tutorial on Statistical Inversion using the Bayesian Paradigm. Note ICES REPORT 12-18, The University of Texas at Austin, The Institute for Computational Engineering and Sciences. http://users.ices.utexas.edu/~tanbui/teaching/Bayesian/Bayesian.pdf.

[30] Tarantola, Albert. 2005. *Inverse Problem Theory and Methods for Model Parameter Estimation*, chap. 1. The General Discrete Inverse Problem, 1–40. Philadelphia, Pennsylvania, USA: Society for Industrial and Applied Mathematics. http://epubs.siam.org/doi/pdf/10.1137/1.9780898717921.ch1.

[31] Trotta, Roberto. 2008. Bayes in the Sky: Bayesian Inference and Model Selection in Cosmology. *Contemporary Physics* 49(2): 71–104. Invited review, https://ned.ipac.caltech.edu/level5/Sept13/Trotta/Trotta_contents.html.

[32] Weber, Charles F, Vladimir A Protopopescu, Michael H Ehinger, Alexander A Solodov, and Catherine E Romano. 2011. Inverse solutions in spectroscopic analysis with applications to problems in global safeguards. In *Proceedings of the Institute of Nuclear Materials Management 52nd Annual Meeting*. Palm Desert, CA, USA. https://www.osti.gov/scitech/biblio/1031530.

[33] Weber, Chuck F, and Bryan L Broadhead. 2006. Inverse depletion/decay analysis using the scale code system. In *Transactions of the American Nuclear Society Winter Meeting*, vol. 95, 248–249. Albuquerque, NM, USA. Track 4: Nuclear and Criticality Safety Technologies.